EUROPEAN LABORATORY FOR PARTICLE PHYSICS

CERN-SPSC-2006-001
SPSC-I-235
January 6, 2006

Letter of Intent

Study of Hadron Production in Collisions of Protons and Nuclei at the CERN SPS

By the participating institutions

electronic version: *http://na49-future.web.cern.ch/na49-future/*

Participating Institutions

University of Athens, Athens, Greece
N. Antoniou, F. Diakonos, A.D. Panagiotou, A. Petridis, M. Vassiliou

University of Bergen, Bergen, Norway
D. Röhrich

KFKI Research Institute for Particle and Nuclear Physics, Budapest, Hungary
L. Boldizsar, Z. Fodor, A. Laszlo, G. Palla, I. Szentpetery, G. Vesztergombi

Cape Town University, Cape Town, South Africa
J. Cleymans

Jagellionian University, Cracow, Poland
Z. Majka, R. Karabowicz, N. Katrynska, P. Staszel

Joint Institute for Nuclear Research, Dubna, Russia
B. Baatar, V. I. Kolesnikov, A. I. Malakhov, G. L. Melkumov

University of Frankfurt, Frankfurt, Germany
M. Gazdzicki, B. Lungwitz, M. Otto, T. Schuster, H. Stroebele

Cern, Geneva, Switzerland
S. Giani, J. Panman

Forschungszentrum Karlsruhe, Karlsruhe, Germany
J. Blumer, R. Engel, A. Haungs, C. Meurer, M. Roth

Świetokrzyska Academy, Kielce, Poland
M. Gazdzicki, R. Korus, St. Mrówczyński, M. Rybczynski, P. Seyboth, G. Stefanek, Z. Wlodarczyk, A. Wojtaszek

Institute for Nuclear Research, Moscow, Russia
F. Guber, A. Kurepin, A. Ivashkin, A. Maevskaya

LPNHE, Universités de Paris VI et VII, Paris, France
B. Andrieu, J. Dumarchez

Pusan Natinal University, Pusan, Republic of Korea
K.-U. Choi, J.-H. Kim, I.-K. Yoo

Faculty of Physics, University of Sofia, Sofia, Bulgaria
D. Kolev, R. Tsenov

St. Petersburg State University, St. Petersburg, Russia
A. G. Asryan, D. A. Derkach, G. A. Feofilov, A. S. Ivanov, R. S. Kolevatov, V. P. Kondratiev, P. A. Naumenko, V. V. Vechernin

State University of New York, Stony Brook, USA
P. Chung, R. Lacey, M. Mitrovski, A. Taranenko

Instituto de Física Corpuscular, IFIC, CSIC and Universidad de Valencia, Valencia, Spain
A. Cervera–Villanueva, J.J. Gómez–Cadenas, M. Sorel

Warsaw University of Technology, Warsaw, Poland
K. Grebieszkow, D. Kikola, W. Peryt, J. Pluta, M. Slodkowski, M. Szuba

University of Warsaw, Warsaw, Poland
E. Skrzypczak

Rudjer Boskovic Institute, Zagreb, Croatia
T. Anticic, K. Kadija, V. Nikolic, T. Susa

contact persons:
Marek Gazdzicki (marek.gazdzicki@cern.ch) and
Gyorgy Vesztergombi (veszter@rmki.kfki.hu)

Contents

1 Introduction

Over the 50 years of CERN history numerous experimental programs were devoted to the study of the properties of strong interactions [1]. Rich data on collisions of hadrons and nuclei were collected. These results together with the data from other world laboratories have significant impact on our understanding of strong interactions and at the same time lead to new questions and define directions of future experimental and theoretical studies [2]. In particular, recently obtained exciting results on nucleus-nucleus collisions from the CERN SPS and the BNL RHIC suggest that the onset of deconfinement is located at low SPS energies. The most important open issues related to this finding are as follows. Is it possible to observe the predicted signals of the onset of deconfinement in fluctuations, anisotropic flow and jet quenching measurements? What is the nature of the transition from the anomalous energy dependence seen in central Pb+Pb collisions at the SPS energies to the smooth dependence observed in p+p interactions? Does the critical point of strongly interacting matter exist and, if it does, where is it located? In addition, rapid development of neutrino and cosmic-ray physics generates an urgent need for precise reference data on hadron production in hadron-nucleus interactions. In particular, the results at the CERN SPS energy range are of high importance.

Therefore, following our previous suggestions [3], we propose to perform a sequence of new measurements of hadron production in collisions of protons and nuclei at CERN by use of the upgraded NA49 apparatus [4]. The proposed program consists of three subjects:

- measurements of hadron production in nucleus-nucleus collisions, in particular fluctuations and long range correlations, with the aim to identify the properties of the onset of deconfinement and search for the critical point of strongly interacting matter,

- measurements of hadron production in proton-proton and proton-nucleus interactions needed as reference data for better understanding of nucleus-nucleus reactions; in particular correlations, fluctuations and high transverse momenta will be the focus of this study,

- measurements of hadron production in hadron-nucleus interactions needed for neutrino and cosmic-ray experiments.

The NA49 apparatus at the CERN SPS served, during the last 10 years, as a very reliable, large acceptance hadron spectrometer and delivered unique high precision experimental data over the full range of SPS beams (from proton to lead) [5, 6] and energies (from 20A GeV to 200A GeV) [7, 8]. Among the most important results from this study is the recent observation [7, 8] of narrow structures in the energy dependence of hadron

production in central Pb+Pb collisions. These structures are located at the low CERN SPS energies ($30A$–$80A$ GeV) and they are consistent with the predictions [9] for the onset of the deconfinement phase transition. The questions raised by this observation serve as a strong motivation for new measurements with nuclear beams at the CERN SPS.

The most efficient and cost effective way to reach the physics goals of the proposed new experimental program is to use the upgraded NA49 detector and its reconstruction software and profit from the experience in physics analysis accumulated over many years.

This document is organized as follows. The physics programme and its motivation are discussed in Section 2. The existing NA49 detector and the required upgrades are described in Section 3. In Section 4 the physics performance is discussed. The beam requirements and expected event rates are given in Section 5. The summary, Section 6, closes the document.

2 Physics Programme

The physics programme of the experimental project is presented according to the increasing physics complexity, level of detector upgrades and availability of the SPS beams. It consists of three subjects:

I. measurements of hadron production in hadron-nucleus interactions needed for neutrino and cosmic-ray experiments,

II. measurements of hadron production in proton-proton and proton-nucleus interactions needed as reference data for better understanding of nucleus-nucleus reactions; in particular correlations, fluctuations and high transverse momenta will be the focus of this study,

III. measurements of hadron production in nucleus-nucleus collisions, in particular fluctuations and long range correlations, with the aim to identify the properties of the onset of deconfinement and search for the critical point of strongly interacting matter.

They will be performed in subsequent stages of the experimental program.

In the following all subjects are presented in detail.

2.1 Neutrino and Cosmic-Ray Physics Needs (I)

2.1.1 Neutrino Physics

Physics Questions and Problems

The study of neutrino oscillation, or in more general terms, the study of neutrino masses and mixings is at present one of the most challenging topics in neutrino physics [10]. From the recent results of neutrino oscillation and other experiments a clear picture emerges of the phenomenology of neutrino mass and mixing. Mixing between the second and third generation neutrinos are found to be close to maximal, while the one between the first and second is large, but not maximal. For the 1–3 mixing only upper limits are available. Recent experiments indicate unique solutions for the values of the 'atmospheric' mass difference (Δm^2_{23}) and the 'solar' mass difference (Δm^2_{12}) in a range such that there are chances to study CP violation in the neutrino sector in the future, provided the value of θ_{13} is large enough.

High-precision measurements of the other angles will provide insight into the mixing mechanism. A combination of a new generation of reactor experiments and the long

baseline experiments T2K [11] and Nova [12] will address these questions in the near future.

The ultimate precision in the measurements of oscillation parameters can be reached by experiments at a neutrino factory. The combination of very intense conventional beams ('super beams') and a 'beta beam' [13], a pure electron(anti)-neutrino beam made by the beta decay of nuclei in a storage ring, can also explore a large range in the parameter space.

As mentioned above, the measurement of the value of θ_{13} is essential to decide if the study of CP violation is within reach at a given facility. A number of experiments are proposed to improve the precision in this parameter. T2K is most probably the first experiment which will probe an entirely new region in this parameter space.

In a long baseline neutrino oscillation experiment, neutrino interactions are measured in a detector far from the neutrino source ('far' in this context means $L/E \gg 1$) and compared with a prediction based on the neutrino flux unmodified by oscillation. A well-known technique to predict the flux is to use a 'near' detector which intercepts the beam at a distance where the effect of oscillations is negligible. If both detectors are sufficiently far from the neutrino source to consider the source point-like and accept the same solid angle, the ratio of the fluxes in the two detectors are accurately predicted by the squared ratio of the distances from the source. When these two conditions are not satisfied the details of the production mechanisms of the beam have to be known. In addition, in the presence of backgrounds, their subtraction requires the knowledge of the neutrino flux spectrum.

In the T2K experiment the neutrino beam is produced using the decays of pions created in the interactions of 30, 40 and 50 GeV/c protons on a carbon target. The pions are then focused into a decay region to produce the neutrinos. (In fact, in T2K, the direction of the neutrino detector is slightly off-axis compared to the pion direction to obtain better properties of the neutrino spectrum.) Apart from a full description of the focusing system, the pion production under the conditions of this experiment has to be known with high precision. In addition to the measurement of pion production it is important to characterize the production of kaons with high accuracy. Decays of kaons are the main component of the electron-neutrino flux which is responsible for the largest background in the measurement of θ_{13}. In the absence of dedicated measurements of hadron production under the specific conditions of the neutrino beam-line, the lack of knowledge of the hadron production introduces a significant systematic error.

HARP Measurement for K2K

The HARP experiment has demonstrated that such a precise measurement of the pion yield as a function of momentum and production angle can reduce the component of the experimental uncertainty introduced by the lack of knowledge of the hadron production to a negligible level [14]. The HARP measurement was performed for the K2K beam,

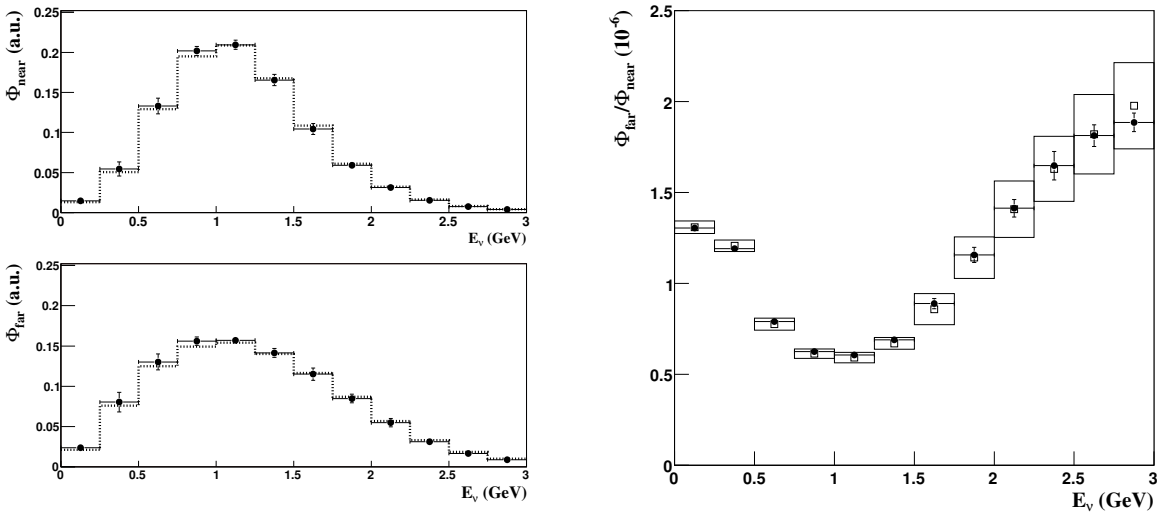

Figure 1: Muon neutrino fluxes in the K2K experiment as a function of neutrino energy E_ν, as predicted by the default hadronic model assumptions in the K2K beam Monte Carlo simulation (dotted histograms), and by the HARP π^+ production measurement (full circles with error bars). The left panel shows unit-area normalized flux predictions at the K2K near (top) and far (bottom) detector locations, $\Phi_{\rm near}$ and $\Phi_{\rm far}$, respectively, while right panel shows the far–to–near flux ratio $\Phi_{\rm far}/\Phi_{\rm near}$ (empty squares with error boxes show K2K model results).

which is produced by a 12.9 GeV/c proton beam impinging on an aluminum target.

The HARP-based prediction has been obtained by substituting the original π^+ production cross-section assumed in the K2K beam Monte Carlo hadronic model with the HARP Sanford-Wang parameterization. All other ingredients of the K2K beam MC simulation, such as primary beam optics, pion re-interactions in the aluminum target, pion focusing, pion decay, etc. were not changed. The Sanford-Wang parameterization [15] of the experimental results provides a smooth extrapolation into regions where no measurements are available. More details on the K2K beam MC assumptions can be found in Ref. [16].

The result of the calculation for the K2K beam is shown in Fig. 1. The left panel shows muon neutrino fluxes in the K2K experiment as a function of neutrino energy E_ν, as predicted by the default hadronic model assumptions in the K2K beam Monte Carlo simulation (dotted histograms), and by the HARP π^+ production measurement (full circles). The plots on that panel show unit-area normalized flux predictions at the K2K near (top) and far (bottom) detector locations, $\Phi_{\rm near}$ and $\Phi_{\rm far}$, respectively. The right panel shows the far–to–near flux ratio $R = \Phi_{\rm far}/\Phi_{\rm near}$ obtained from the K2K

Monte Carlo (empty squares with error boxes) and from the HARP measurement (full circles with error bars). The fluxes predicted by HARP and the present K2K model are in good agreement within the errors. This is reflected also in a good agreement in R, in particular in the oscillation region (below 1.5 GeV). The error in R propagating the uncertainties of the HARP measurement is of the order of 1%. The current systematic error attached to R in the K2K analysis is of the order of 7%. It clearly shows the considerable improvement that can be achieved by K2K by using this new measurement. It should be noted however, that part of the latter uncertainty is also associated with additional uncertainties in the flux calculations.

The recent HARP results are compared with the collection of π^+ production data from aluminum targets available in the literature prior to the HARP measurement [18, 19, 20, 21]. The comparison is restricted to proton beam momenta between 10 and 15 GeV/c (close to the K2K beam momentum of 12.9 GeV/c), and for pion polar angles below 200 mrad (the range measured by HARP and of relevance to K2K).

In order to match pion momenta and angles measured in the different experiments the comparison is based on the HARP Sanford-Wang parameterization. A correction to rescale the HARP Sanford-Wang parameterization at 12.9 GeV/c beam momentum to the momenta in the range 10 GeV/c–15 GeV/c beam momenta of the other Al datasets is applied [22].

Figure 2 shows the comparison between HARP and the above datasets. The figure shows that it is of enormous importance to measure the full phase-space in a single experiment to avoid the relatively large systematic normalization errors between the different experiments. The situation for the T2K experiment is analogous, certainly for the first phase of the data taking. (In a possible second phase an extra detector could be constructed at an intermediate distance, which is sensitive to a neutrino flux with properties much closer to the flux at the far detector.) As mentioned above, the conditions under which the beam will be produced is different from the case of K2K, and therefore new pion production measurements are needed. The requirements are similar to the ones for the K2K measurement. Since, in addition to the measurement of the disappearance of muon neutrinos also the appearance of electron neutrinos is important, the kaon production yield is an important element to determine the beam backgrounds.

Several opportunities to measure the pion yield for the beam line of the T2K experiment have been explored: the COMPASS experiment at CERN, the MIPP experiment at Fermilab, and the NA49 experiment at CERN. The most promising option is the use of the NA49 detector.

This detector has the acceptance and the particle ID capabilities needed for this measurement. In the following these capabilities will be compared with the requirements imposed by the T2K beam-line.

In order to demonstrate the relevance of the hadron production measurements, one can investigate which hadron decays contribute to the neutrino flux in the T2K detectors. The relevant region in the p–θ plane, where p and θ are the momentum and angle of pions

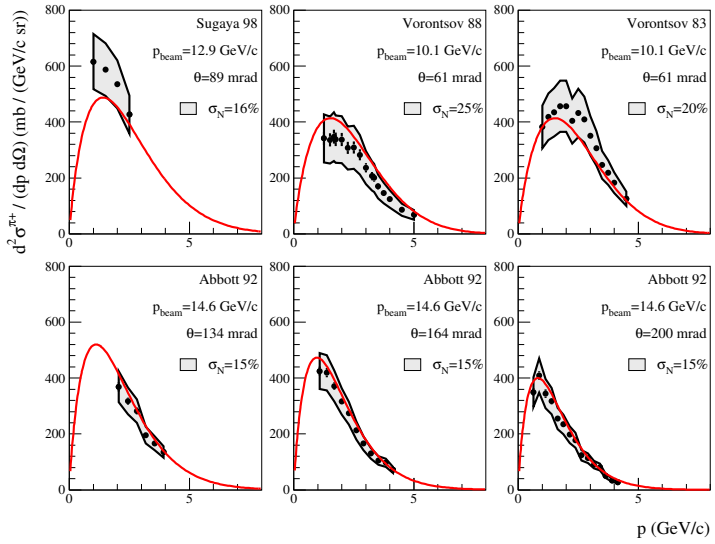

Figure 2: Comparison of the double-differential pion production cross-section measured in HARP, and the one measured in past experiments using an aluminum target and 10-15 GeV/c momentum beam protons. The points are the data from the experiments prior to HARP, and the shaded area reflect their normalization uncertainty. The solid line is the HARP Sanford-Wang parameterization rescaled to the beam momentum of past experiments, as discussed in the text.

at their production point, respectively, is shown in Fig. 3. In this figure the size of the boxes is a measure of the relevance of a given point in the hadron production phase space. The population in this plane can be compared with the performance of NA49 detector (see Section 4.1), which is seen to provide full coverage of the relevant phase space region.

Physics Needs

It is foreseen to operate the T2K beam-line initially with 30 GeV/c protons, while upgrades to 40 GeV/c and 50 GeV/c are foreseen. It is planned to use a carbon production target. The most important data-sets would be taken with a thin carbon target (a few per cent of a nuclear interaction length $\lambda_{\rm I}$ which would be used to measure the primary p–C hadron production cross-section). In addition to this basic configuration, also runs with targets of various thicknesses (of the order of one $\lambda_{\rm I}$) would be needed to control the simulation of secondary interactions.

If time permits, different materials which could be envisaged for targets in higher intensity operation should be added.

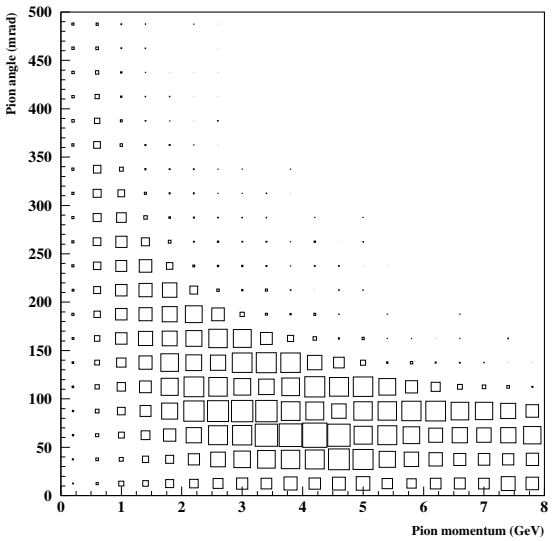

Figure 3: The population in the p–θ plane of pions of which the decay contributes to the neutrino flux in the T2K detectors. The size of the boxes indicates the relative contribution of a given point in phase space.

2.1.2 Cosmic-Ray Physics

Physics Questions and Problems

One of the central questions of astroparticle physics is that of the sources and propagation of cosmic rays. Even more than 90 years after the discovery of cosmic rays we still don't know their elemental composition at high energy and also the information on the energy spectrum is very limited [23, 24]. Knowing the cosmic-ray composition is the key to understanding phenomena such as the *knee* – a change in the power-law index of the cosmic ray flux at about 3×10^6 GeV – and the transition from galactic to extra-galactic cosmic rays. Furthermore, composition information is essential for confirming or ruling out models proposed for the sources of ultra-high energy cosmic rays, many of which postulate new particle physics [25].

At energies above 10^5 GeV, the flux of cosmic rays is so low that it cannot be measured directly using particle detectors. Therefore all cosmic-ray measurements of higher energy are based on analyzing the secondary particle showers, called extensive air showers, which they produce in the atmosphere of the Earth. To interpret the characteristics of extensive air showers in terms of primary particle type and energy, detailed modelling of the various interaction and decay processes of the shower particles is needed [26]. Modern high-precision experiments like KASCADE [27] and the Pierre Auger Observatory [28]

measure several observables for each shower. The uncertainty in interpreting the data from these experiments is dominated by the uncertainty in predicting hadronic multi-particle production in extensive air showers.

For example, the KASCADE Collaboration uses the measured number of electrons and muons at detector level to derive the primary energy and composition of the showers in the knee energy region. Having collected more than 40 million showers it is still not possible to obtain a clear picture of the elemental composition [29]. Applying different hadronic interaction models leads to significantly different fluxes for the elemental groups considered in the analysis. In particular, the fundamental question of having a mass- or rigidity-dependent scaling of the knee positions of the individual flux components cannot be answered.

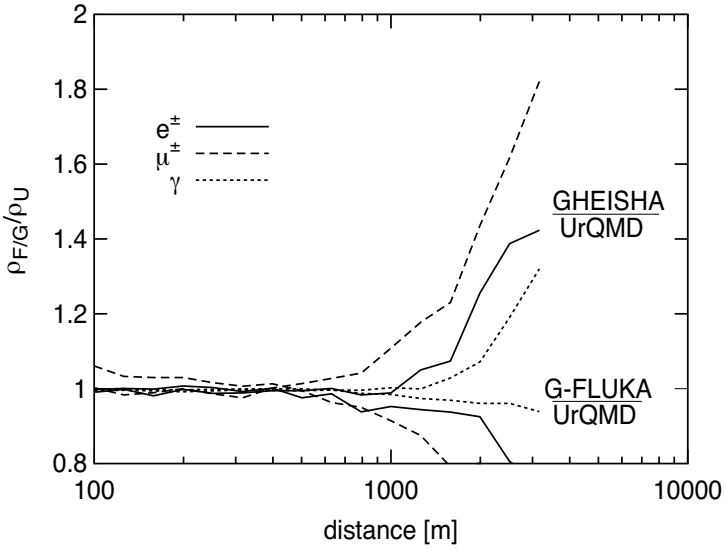

Figure 4: Lateral distribution of particles (electrons, photons and muons) in vertical, proton-induced showers of 10^{10} GeV. Interactions at laboratory energies below 80 GeV were simulated with the models G-FLUKA [30], UrQMD [31], and GHEISHA [32]. The model QGSJET [33] was used for simulating high energy interactions. Shown is the ratio of the particle densities relative to the prediction of UrQMD. (from [34])

The dependence on modelling hadronic interactions is also clearly demonstrated by the fact that the Auger Collaboration finds indications of a 20% discrepancy of the energy that would be assigned to a shower by using either only the Auger surface detector data or the calorimetric measurement of the Auger fluorescence telescopes [35]. In addition, any composition analysis will be hampered by the uncertainty of simulating hadronic interactions. For example, the slope of the lateral distribution of particles in a shower is a measure of the mass of the primary particle. This slope, however, is also very sensitive to assumptions on hadronic multi-particle production in the energy range up to a few

hundred GeV, see Fig. 4.

In the foreseeable future soft multi-particle production will not be calculable within QCD. Therefore the modelling of cosmic-ray interactions will strongly depend on the input from accelerator experiments.

Role of low-energy hadron production in air showers

Typically only the dependence of extensive air shower predictions on the characteristics of hadronic interactions at high energy is considered [36]. Only recently is has been realized that interactions in the energy range up to a few hundred GeV are also very important. This applies in particular to shower particles measured at large lateral distance, as is the case in air shower arrays [37, 38].

In the following we illustrate the role of low-energy interactions by considering muon production in extensive air showers [39]. (It should be kept in mind that the ratio of muons to electrons in a shower is one of the best composition-sensitive observables.) The simulations are done for proton showers of 10^6 GeV but the results apply also to showers of higher energy and other hadronic primary particles. The competing processes of pion interaction and decay in an air shower lead to a relatively energy-independent typical energy below which pions decay and produce muons.

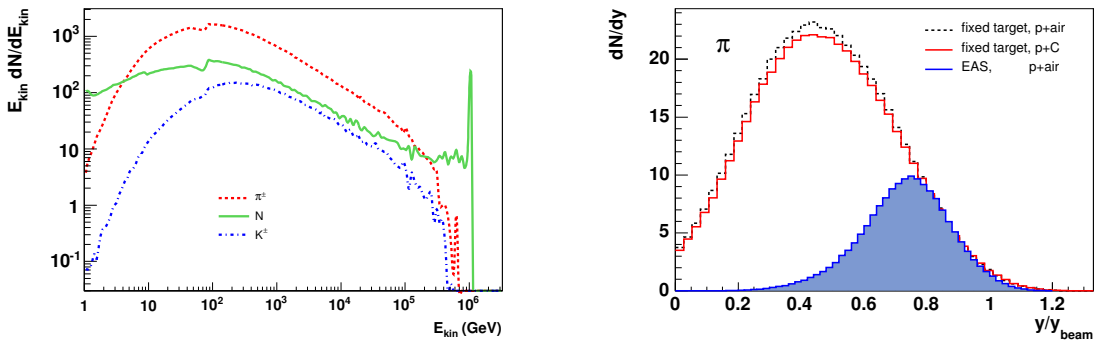

Figure 5: Left panel: Energy distribution of interactions in a shower which produce a meson that in turn decays into an observable muon. The discontinuity at 80 GeV (where the hadronic interaction model is switched from GHEISHA to QGSJET) reflects shortcomings in the hadronic interaction models. The three curves show the relative importance of pion, kaon and nucleon interactions. Right panel: Rapidity distribution (relative to beam rapidity) of secondary pions which produce muons that are detected in air shower experiments. The minimum-bias pion distribution is shown for reference and compared to that of proton-carbon interactions. (from [39])

In Fig. 5 (left) the energy distribution of hadronic interactions, in which at least one

meson was produced that in turn decayed to a muon that reached sea level, is shown. The maximum of the energy distribution falls in the range between 80 and 200 GeV. Most of the interactions are induced by pions (70%) and nucleons (20%). The shortcomings of the simulation of hadronic interactions are clearly visible as a discontinuity between the energy region of the high- and low-energy models applied in this simulation.

The rapidity distribution of the secondary particles, measured relative to the rapidity of the particle that initiated the interaction, is shown in Fig. 5 (right). The constraint on the muon energy (low-energy muons decay before reaching the detector level) leads to a strong preference for high energy pions in air showers (filled histogram). Details about the simulation and further phase space comparisons can be found in [39].

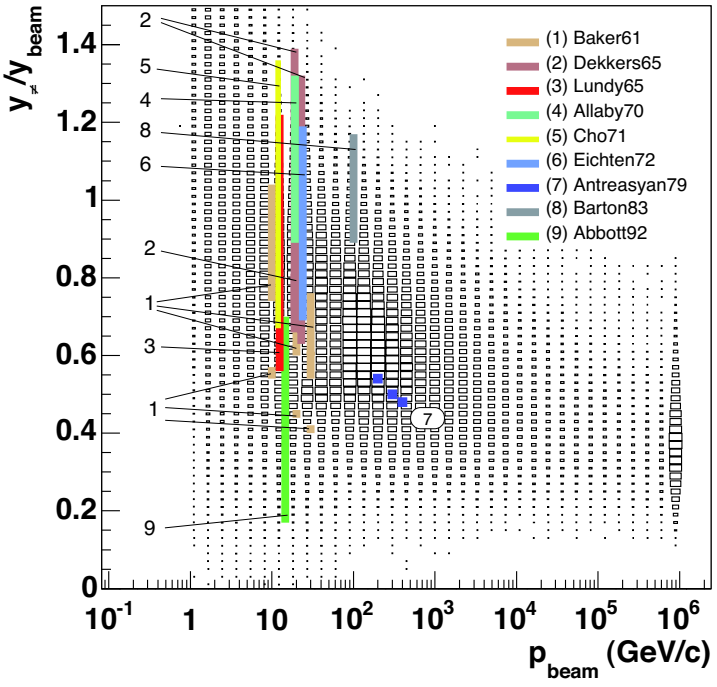

Figure 6: Compilation of existing data on pion production in proton collisions with light nuclei [40]. The covered secondary particle phase space is indicated by the shaded regions. The histogram shows the relative importance of the beam energy and secondary particle rapidity for muon production in extensive air showers.

There is a lack of measurements covering the aforementioned energy range and secondary particle phase space. A compilation of available measurements for proton projectiles is shown in Fig. 6. Moreover, there exist no data for pion projectiles with good phase

space coverage for light target nuclei.

Both the energy as well as the secondary particle phase space accessible with the NA49 detector setup are of great importance for air shower physics. In particular the excellent forward acceptance and particle identification are unique features needed for performing measurements that can be used in air shower simulations.

Physics Needs

Regarding cosmic-ray physics, the most important projectile-target combinations would be pion and proton beams on a carbon target. Beam energies as high as 150 GeV would be desirable, but 50 GeV would already reduce model uncertainties considerably. All the data have to be taken with minimum bias trigger and thin targets. It should be mentioned that the analysis of HARP p/π-carbon data at lower energy (3 GeV to 15 GeV) is in progress.

2.2 Reference p+p and p+A data (II)

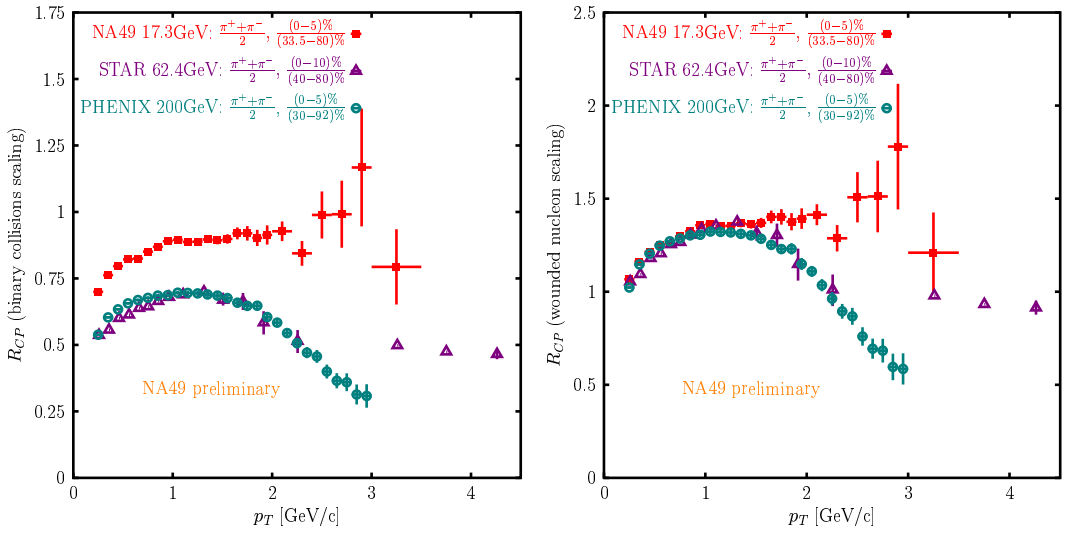

Figure 7: The ratio (R_{CP}) of pion transverse momentum spectra of central to peripheral Pb+Pb interactions at 158A GeV as measured by NA49 [41] scaled by the number of binary collisions (left) and wounded nucleons (right).

An interpretation of the rich experimental results on nucleus-nucleus collisions at high energies (see e.g. Section 2.3 in this document) relies to a large extent on a comparison to the corresponding data on p+p and p+A interactions. However, the available p+p and p+A results concern mainly basic properties of hadron production and they are sparse.

Many needed data on fluctuations, correlations and, in particular, particle production at high transverse momenta are missing. Thus the measurements of hadron production in p+p and p+A reactions are necessary and should be performed in parallel to the corresponding measurements for A+A collisions. In the following this general requirement is illustrated by an important example, the inclusive spectra of identified hadrons at high transverse momentum, p_T.

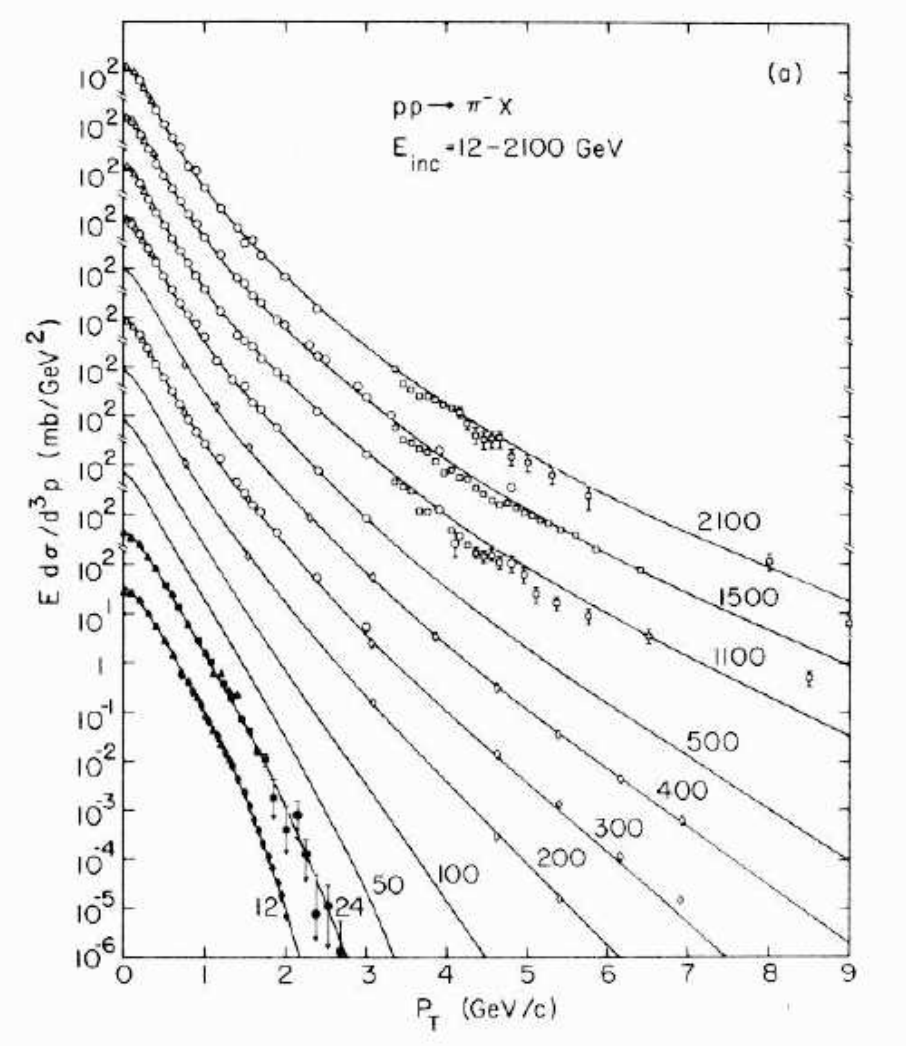

Figure 8: A compilation of the transverse momentum spectra of negatively charged pions produced in p+p interactions at different collision energies [42]. The energy values are given in the laboratory system. There are no data points between 24 GeV and 200 GeV.

One of the most striking features observed at BNL-RHIC is the suppression of high

p_T hadron production in central A+A collisions relative to peripheral A+A collisions or p+p interactions.

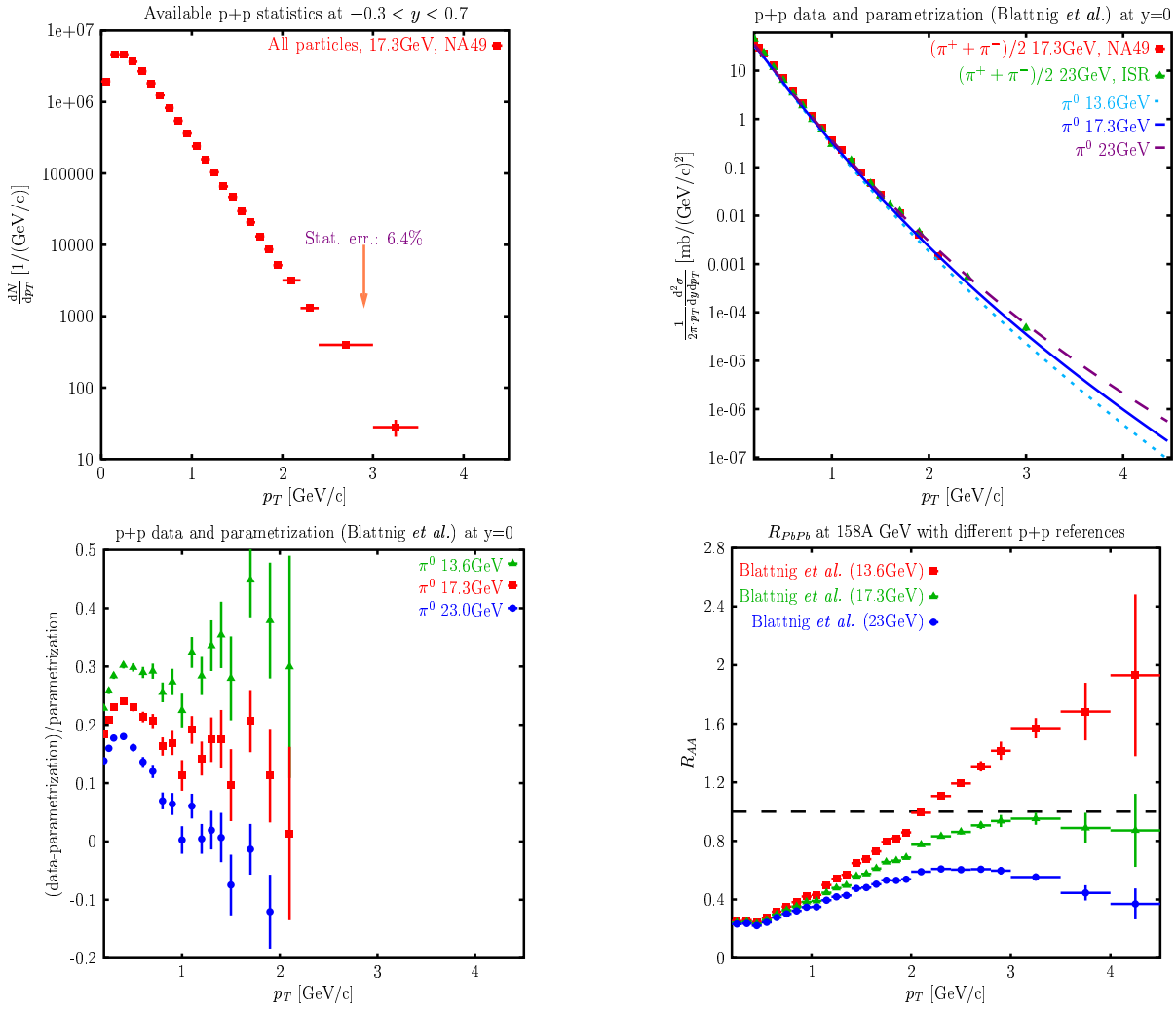

Figure 9: Top/left: Uncorrected transverse momentum spectrum of all charged hadrons as registered by NA49 in $4 \cdot 10^6$ p+p interactions at 158 GeV. Top/right: Data points show the corrected p_T spectra of pions produced in p+p interactions at energies close to 158 GeV (the top SPS energy for Pb+Pb collisions) in comparison to curves depicting the Blattnig et al. [43] parameterization calculated for three slightly different values of the energy parameter, corresponding to the present uncertainty in the extrapolation of existing p+p data. Bottom/left: The deviations of the measured p_T spectrum at 158 GeV from the Blattnig et al. parameterizations. Bottom/right: The R_{AA} ratio calculated for central Pb+Pb collisions at 158A GeV using the Blattnig et al. parameterizations of the p+p data.

This is generally interpreted as a sign of parton energy loss in hot and dense hadronic matter created at the early stage of nucleus-nucleus collisions. This interpretation implies that the suppression should disappear at low energies where the energy density is not enough for creation of the deconfined state of matter. Numerous results on energy dependence of hadron yields and spectra indicate that the onset of deconfinement is located at the low SPS energies (see Section 2.3). Thus it is crucial to extend the study of the energy dependence to high p_T production, in particular in the CERN SPS energy range, to search for onset phenomena in the high p_T region.

The NA49 and other CERN SPS experiments measured identified hadron production in Pb+Pb collisions at 158A GeV up $p_T \approx$ 3-4 GeV/c [41]. The first results expressed in terms of the ratio of the p_T spectra measured in central and peripheral collisions (R_{CP}) are shown in Fig. 7 where the corresponding results at RHIC energies are also plotted for comparison. The suppression seems to weaken gradually with decreasing collision energy. The key measure in this study is, however, the ratio between p_T spectra measured in central Pb+Pb collisions and p+p interactions, R_{AA}.

A compilation of the p_T spectra of pions produced in p+p interactions (excluding NA49 data) is shown in Fig. 8 which suggests a strong energy dependence of the high p_T tail over the SPS energy range, where the data points are missing. The statistics of the NA49 p+p published data ($\approx 3 \cdot 10^6$ events) at 158 GeV is presented in Fig. 9, it ends at about 2 GeV/c. All this leads to a large systematic uncertainty of the estimate of the high p_T tail of the p+p spectrum based on an extrapolation of the existing data, see Fig. 9 for an illustration.

The above example clearly shows an important need for high statistics and high precision measurements of identified hadron production in p+p and p+A collisions at SPS energies. They require a significant increase, by a factor of about 10-50, of the event collection rate.

2.3 Onset of deconfinement and critical point in A+A collisions (III)

2.3.1 Key questions

One of the key issues of contemporary physics is the understanding of strong interactions and in particular the study of the properties of strongly interacting matter in equilibrium. What are the phases of this matter and how do the transitions between them look like are questions which motivate a broad experimental and theoretical effort. The study of high energy nucleus-nucleus collisions gives us a unique possibility to address these questions in well-controlled laboratory experiments.

Onset of Deconfinement

Recent results on the energy dependence of hadron production in central Pb+Pb collisions at 20A, 30A, 40A, 80A and 158A GeV coming from the energy scan program at the CERN SPS serve as evidence for the existence of a transition to a new form of strongly interacting matter, the Quark Gluon Plasma (QGP) in nature. Thus they are in agreement with the conjectures that at the top SPS and RHIC energies the matter created at the early stage of central Pb+Pb (Au+Au) collisions is in the state of QGP.

The key results are summarized in Fig. 10. The most dramatic effect can be seen in the energy dependence of the ratio $\langle K^+\rangle/\langle\pi^+\rangle$ of the mean multiplicities of K^+ and π^+ produced per event in central Pb+Pb collisions, which is plotted in the top panel of the figure. Following a fast threshold rise, the ratio passes through a sharp maximum in the SPS range and then seems to settle to a lower plateau value at higher energies. Kaons are the lightest strange hadrons and $\langle K^+\rangle$ is equal to about half of the number of all anti-strange quarks produced in the collisions. Thus, the relative strangeness content of the produced matter passes through a sharp maximum at the SPS in nucleus-nucleus collisions. This feature is not observed for proton-proton reactions.

A second important result is the constant value of the apparent temperature observed in the transverse momentum distributions of K^+ mesons in central Pb+Pb collisions at SPS energies as shown in the bottom panel of the figure. The plateau at the SPS energies is preceeded by a steep rise of the apparent temperature at the AGS and followed by a further increase indicated by the RHIC data. Very different behavior is measured in proton-proton interactions.

Presently, the sharp maximum and the following plateau in the energy dependence of the relative strangeness content has only been reproduced by the statistical model of the early stage [9] in which a first order phase transition is assumed. In this model the maximum reflects the decrease in the number ratio of strange to non-strange degrees of freedom and changes in their masses when deconfinement sets in. Moreover, the observed steepening of the increase in pion production with collision energy is consistent with the expected excitation of the quark and gluon degrees of freedom. Finally, in the picture of the expanding fireball, the apparent temperature is related to the thermal motion of the particles and their collective expansion velocity. Collective expansion effects are expected to be important only in heavy ion collisions as they result from the pressure generated in the dense interacting matter. The stationary value of the apparent temperature of K^+ mesons may thus indicate an approximate constancy of the early stage temperature and pressure in the SPS energy range due to the coexistence of hadronic and deconfined phases, as in the case of first order phase transition [50, 51].

Thus, the anomalies in the energy dependence of hadron production in central Pb+Pb collisions at low SPS energies serve as evidence for the onset of deconfinement and the existence of QGP in nature. They are consistent with the hypotheses that the observed transition is of first order. The anomalies are not observed in p+p interactions and they

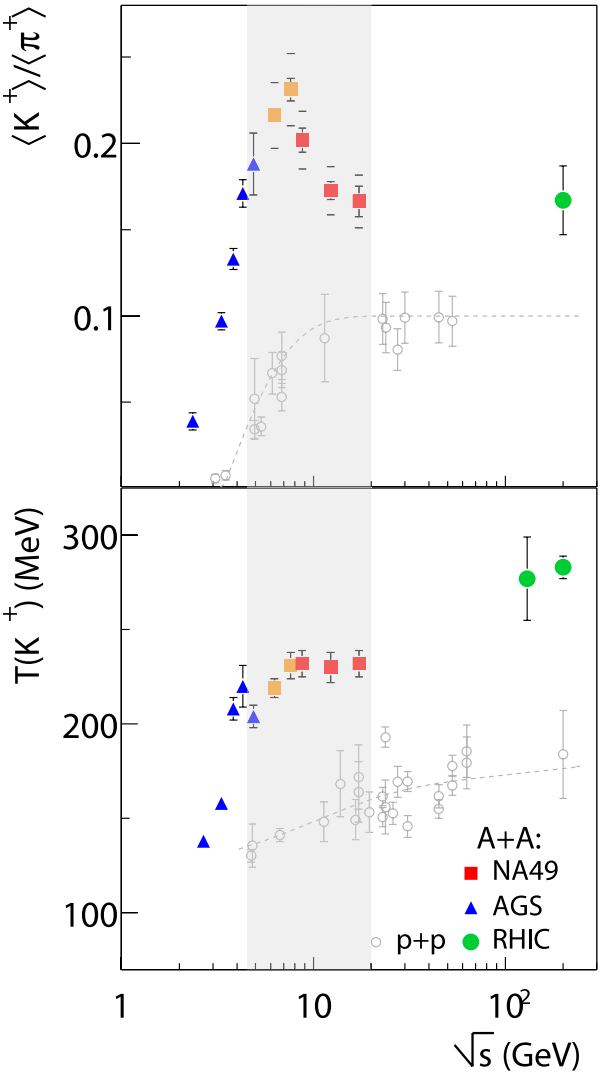

Figure 10: Collision energy dependence of the K^+ to π^+ ratio and the inverse slope parameter of the transverse mass spectra measured in central Pb+Pb and Au+Au collisions (solid symbols) compared to results from p+p reactions (open dots). The changes in the SPS energy range (solid squares) suggest the onset of the deconfinement phase transition. The energy region covered by the future measurements at the CERN SPS is indicated by the gray band.

are not reproduced within hadronic models [52].

These results and their interpretation raise numerous questions which can be answered

only by new measurements. Two most important open problems are:

- **is it possible to observe the predicted signals of the onset of deconfinement in fluctuations [53] and anisotropic flow [54]?**
- **what is the nature of the transition from the anomalous energy dependence measured in central Pb+Pb collisions at SPS energies to the smooth dependence measured in p+p interactions?**

Critical Point

In the letter of Rajagopal, Shuryak, Stephanov and Wilczek addressed to the SPS Committee one reads: ... *Recent theoretical developments suggest that a key qualitative feature, namely a critical point (of strongly interacting matter) which in sense defines the landscape to be mapped, may be within reach of discovery and analysis by the SPS, if data is taken at several different energies. The discovery of the critical point would in stroke transform the map of the QCD phase diagram which we sketch below from one based only on reasonable inference from universality, lattice gauge theory and models into one within a solid experimental basis.* ... More detailed argumentation is presented below.

Rich systematics of hadron multiplicities produced in nuclear collisions can be reasonably well described by hadron gas models [55, 56, 57]. Among the model parameters fitted to the data are temperature, T, and baryonic chemical potential, μ_B, of the matter at the stage of freeze-out of the hadron composition (the chemical freeze-out). These parameters extracted for central Pb+Pb collisions at the CERN SPS energies are plotted in Fig. 11 together with the corresponding results for higher (RHIC) and lower (AGS, SIS) energies. With increasing collision energy T increases and μ_B decreases. A rapid increase of temperature is observed up to mid SPS energies, from the top SPS energy ($\sqrt{s_{NN}} =$ 17.2 GeV) to the top RHIC energy ($\sqrt{s_{NN}} = 200$ GeV) the temperature increases only by about 10 MeV.

The sketch of the phase diagram of strongly interacting matter in the $(T - \mu_B)$ plane as suggested by QCD-based considerations [58, 59] is shown in Fig. 11. To a large extent these predictions are qualitative, as QCD phenomenology at finite temperature and baryon number is one of the least explored domains of the theory. More quantitative results come from lattice QCD calculations which can be performed at $\mu_B = 0$. They strongly suggest a rapid crossover from the hadron gas to the QGP at the temperature $T_C = 170 - 190$ MeV [60, 61], which seems to be somewhat higher than the chemical freeze-out temperatures of central Pb+Pb collisions ($T = 150 - 170$ MeV) [62] at the top SPS and RHIC energies.

The nature of the transition to QGP is expected to change with the increasing baryochemical potential. At high potential the transition may be of the first order, with the end point of the first order transition domain, marked E in Fig. 11, being the critical point of the second order. Recently even richer structure of the phase transition to QGP was

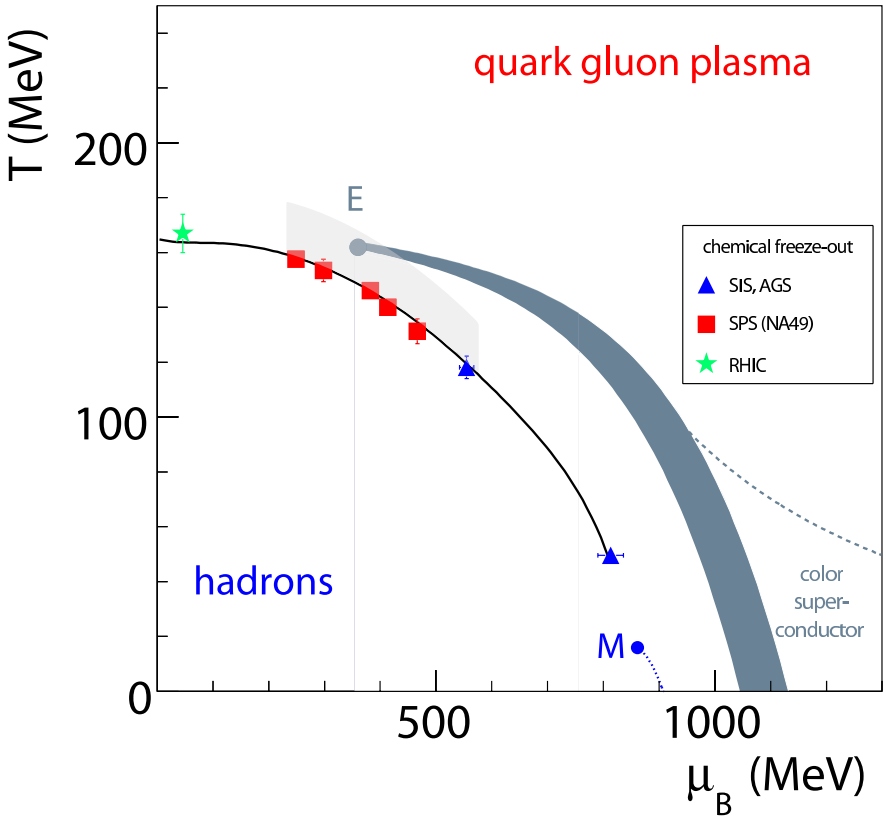

Figure 11: The hypothetical phase diagram of strongly interacting matter in the plane temperature, T, and baryonic chemical potential, μ_B. The end point **E** of the first order transition strip is the critical point of the second order. The chemical freeze-out points extracted from the analysis of hadron yields in central Pb+Pb (Au+Au) collisions at different energies are plotted by the solid symbols. The region covered by the future measurements at the CERN SPS is indicated by the gray band.

discussed within a statistical model of quark gluon bags [63]. It was suggested that the line of the first order phase transition at high μ_B is followed by the line of the second order phase transition at intermediate μ_B, and then by the lines of "higher order transitions" at low μ_B. A characteristic property of the second order phase transition (the critical point or line) is a divergence of the susceptibilities. Consequently an important test for a second-order phase transition at the critical point is the validity of appropriate power laws in measurable quantities related to critical fluctuations. Techniques associated with such measurements in nuclear collisions have been developed recently [64] with emphasis on the sector of isoscalar di-pions (σ-mode) as required by the QCD conjecture for the

critical end point in quark matter [58]. Employing such techniques in a study of nuclear collisions at different energies at the SPS and with nuclei of different sizes, the experiment may test not only the existence and location of the critical point but also the size of critical fluctuations as given by the critical exponents of the QCD conjecture.

Thus when scanning the phase diagram a maximum of fluctuations located in a domain close to the critical point ($\Delta T \approx 15$ MeV and $\Delta\mu_B \approx 50$ MeV [65]) or the critical line should signal the second order phase transition. The position of the critical region is uncertain, but the best theoretical estimates based on lattice QCD calculations locate it at $T \approx 158$ MeV and $\mu_B \approx 360$ MeV [66, 67] as indicated in Fig. 11. It is thus in the vicinity of the chemical freeze-out points of central Pb+Pb collisions at the CERN SPS energies.

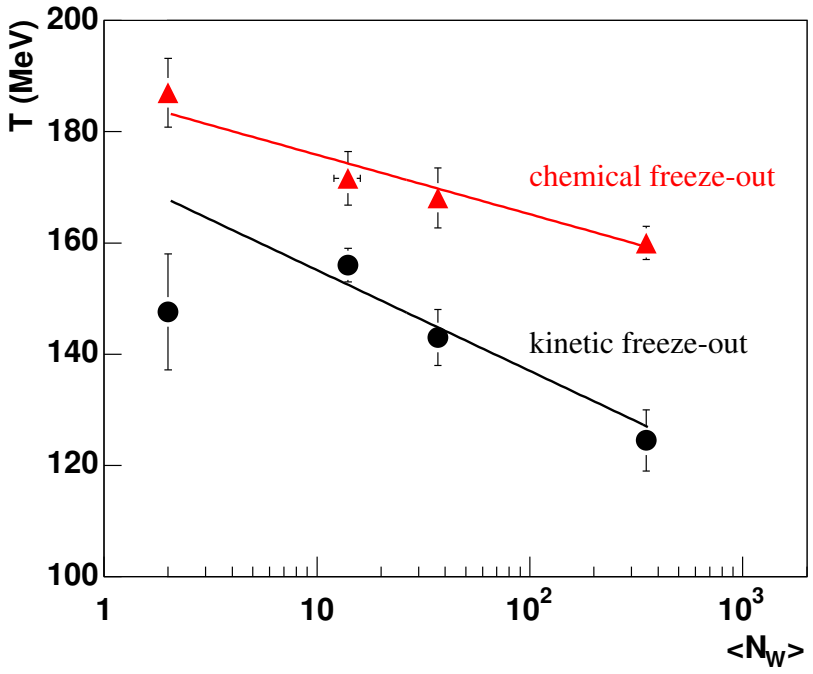

Figure 12: The dependence of the chemical and kinetic freeze-out temperatures on the mean number of wounded nucleons for p+p, C+C, Si+Si and Pb+Pb collisions at 158A GeV.

Pilot data [5] on interactions of light nuclei (Si+Si, C+C and p+p) taken by NA49

at $40A$ and $158A$ GeV indicate that the freeze-out temperature increases with decreasing mass number, A, of the colliding nuclei, see Fig. 12. This means that a scan in the collision energy and mass of the colliding nuclei allows us to scan the $(T - \mu_B)$ plane in a search for the critical point (line) of strongly interacting matter [68].

The experimental search for the critical point by investigating nuclear collisions is justified at energies higher than the energy of the onset of deconfinement. This is because the energy density at the early stage of the collision, which is required for the onset of deconfinement is higher than the energy density at freeze-out, which is relevant for the search for the critical point. The only anomalies possibly related to the onset of deconfinement are measured at $\sqrt{s_{NN}} \approx 8$ GeV (see Fig. 10). This limits a search for the critical point to an energy range $\sqrt{s_{NN}} > 8$ GeV. Fortunately, as discussed above and illustrated in Fig. 11, the best theoretical predictions locate the critical point in the $(T - \mu_B)$ region accessible in nuclear collisions in this energy range. Thus the new measurements at the CERN SPS can answer the fundamental question:

- **does the critical point of strongly interacting matter exist in nature and, if it does, where is it located?**

In conclusion, the recent experimental and theoretical findings strongly suggest that a further study of nuclear collisions in the CERN SPS energy range is of particular importance. The new measurements can answer the questions concerning the nature of the onset of deconfinement and the existence and location of the critical point.

2.3.2 General requirements

The physics goals of the new experimental program with nuclear beams at the CERN SPS presented in the previous section require an energy scan in the whole SPS energy range ($10A$-$200A$ GeV) with light and intermediate mass nuclei. The measurements should be focused on the precise study of fluctuations and anisotropic flow. The first NA49 results on these subjects [69, 70, 71, 72] suggest, in fact, the presence of interesting effects for collisions with moderate number of participant nucleons and/or at low collision energies. However, a very limited set of data and serious resolution and acceptance limitations do not allow firm conclusions. This will be discussed in detail in Section 4.1.

The general physics needs when confronted with the existing NA49 results and experience suggest improvements of the current performance of the NA49 apparatus.

1. The event collection rate should be significantly increased in order to allow a fast collection of sufficient statistics for a large number of different reactions (A, $\sqrt{s_{NN}}$).

2. The resolution in the event centrality determination based on the measurement of the energy of projectile spectator nucleons should be improved. This is important for high precision measurements of event-by-event fluctuations.

3. The acceptance for the measurements of charged hadrons has to be increased and made as uniform as possible.

With such an improved setup we intend to register C+C, Si+Si and In+In collisions at $10A$, $20A$, $30A$, $40A$, $80A$, $158A$ GeV and a typical number of recorded events per reaction of $2 \cdot 10^6$.

In the following sections we propose hardware upgrades of the NA49 apparatus (Sections 3.3 and 3.4) and discuss the resulting improvements of its physics performance (Sections 4.3). The detailed beam requirements and the expected event rates are presented in Section 5.

2.3.3 Experimental landscape

High energy nucleus-nucleus collisions have been studied experimentally since the beginning of the 1970s in several international and national laboratories. Several groups participating in this letter of intent have a long experience in this study. In particular, pioneering measurements of hadron production were performed by: the Dubna, Moscow (a first measurement of the charged kaon to pion ratio [73]), and Warsaw groups at the Dubna synchrophasotron, the Stony Brook group at the BNL AGS, the Athens, Bergen, Dubna and Frankfurt groups at the CERN SPS and the Bergen, Cracow and Frankfurt groups at the BNL RHIC.

Present and future accelerator facilities for relativistic nuclear beams are shown in Fig. 13, where their nominal energy range is also indicated. The facilities are ordered according to the top collision energy in Fig. 14. The basic physics of strongly interacting matter which is related to the specific energy domain is also given in Fig. 14.

In addition to the CERN SPS also the BNL RHIC [74] can study the physics of the onset of deconfinement and the critical point. Up to now the experiments at RHIC were performed in the collider mode in the energy range $\sqrt{s_{NN}} = 20 - 200$ GeV. It seems, however, plausible to run RHIC even at significantly lower energies [75], down to $\sqrt{s_{NN}} \approx 5$ GeV, and thus cover the SPS energy range. The advantages of this potential RHIC program would be:

- an even broader collision energy range covered by a single experimental facility which yields small relative systematic errors of the resulting energy dependence of hadron production properties,

- a uniform and almost complete acceptance around mid-rapidity, provided the existing STAR apparatus is used in this study; this uniform acceptance is important for the measurements of the anisotropic flow.

However, running experiments in the collider mode does not allow a measurement of the spectator fragments which is important for studies of event-by-event fluctuations, in particular of extensive variables like particle multiplicity.

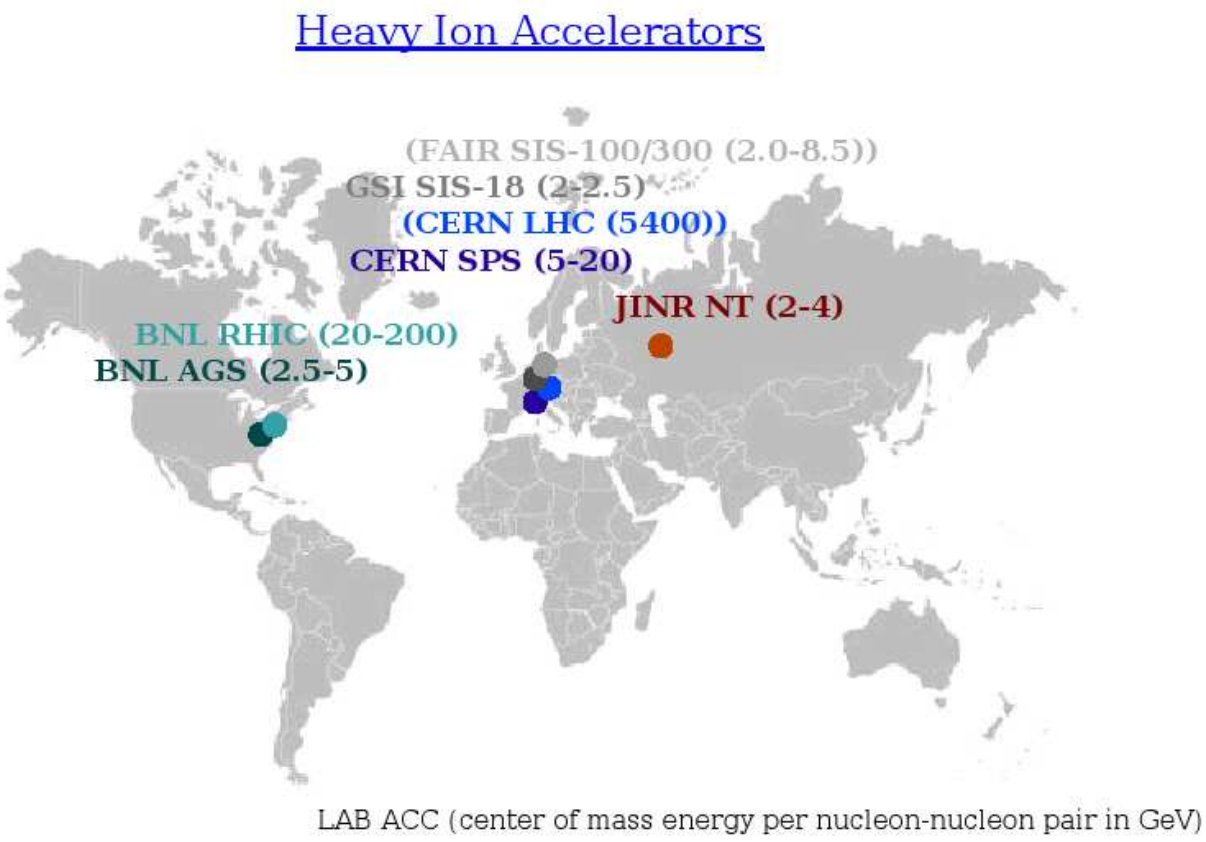

Figure 13: The present and future accelerators of relativistic nuclear beams. For each facility the name of the laboratory, the name of the accelerator and the energy range (center of mass energy per nucleon-nucleon pair in GeV) are given.

The RHIC accelerator can be used also as a fixed target machine. In this case the top energy is $\sqrt{s_{NN}} \approx 14$ GeV and the existing BRAHMS detector can be used for measurements of inclusive identified hadron spectra [74]. This option is considered as a possible fast cross-check of the NA49 results.

In view of the importance of the physics of the onset of deconfinement and the critical point it appears desirable to perform the experiments both at the SPS and RHIC. The expected results will be complementary in the important aspects of fluctuations and anisotropic flow. The partial overlap of the results will allow the necessary experimental cross-checks.

A future CBM experiment at SIS-300 (FAIR, Darmstadt) will study properties of

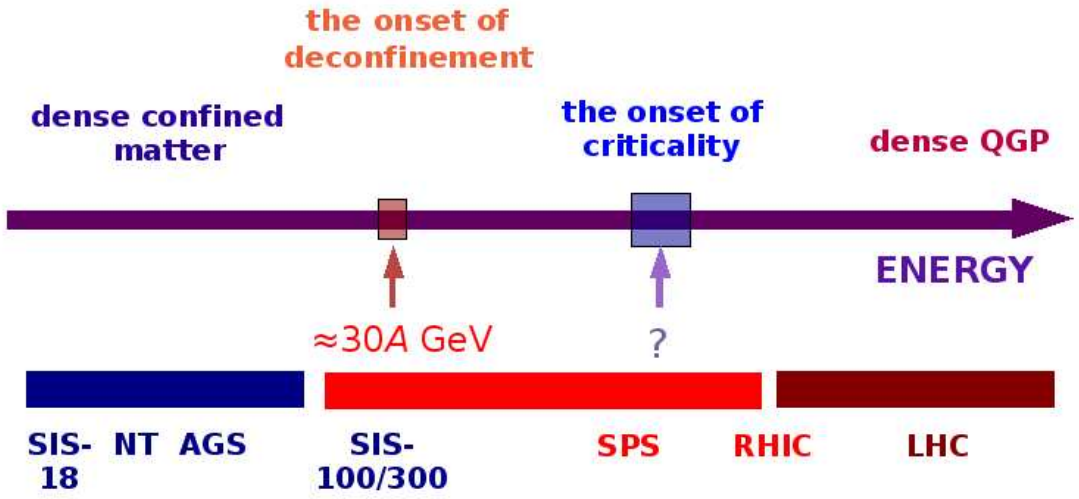

Figure 14: The accelerators of relativistic nuclear beams ordered according to the top collision energy and the basic physics of strongly interacting matter related to a given energy domain. The central horizontal bar indicates the energy range of the CERN SPS.

dense baryonic matter in nuclear collisions at energies 10A-40A GeV starting from 2015. It will be able to measure low cross-section processes like di-lepton as well as open and hidden charm hadron production. Both experiments have several collaborating institutions and groups in common, some of which have embarked on a common project for the construction of a Projectile Spectator Detector (see Section 3.4.1). Others work together in a Virtual Institute (VI-SIM) of the Helmholtz Gemeinschaft.

3 Experimental Apparatus

3.1 NA49 detector

The NA49 experiment is a large acceptance hadron spectrometer at the CERN-SPS for the study of the hadronic final states produced by collisions of various beam particles (p, Pb from the SPS and C, Si from the fragmentation of the primary Pb beam) with a variety of fixed targets. The main tracking devices are four large volume Time Projection Chambers (TPCs) (Fig. 15) which are capable of detecting 70% of the approximately 1500 charged particles created in a central Pb+Pb collision at 158A GeV. Two of them, the vertex TPCs (VTPC-1 and VTPC-2), are located in the magnetic field of two superconducting dipole magnets (1.5 and 1.1 T, respectively) and two others (MTPC-L and

MTPC-R) are positioned downstream of the magnets symmetrically to the beam line. The NA49 TPCs allow precise measurements of particle momenta p with a resolution of $\sigma(p)/p^2 \cong (0.3 - 7) \cdot 10^{-4}$ (GeV/c)$^{-1}$. The set–up is supplemented by two time of flight (TOF) detector arrays with a time measurement resolution $\sigma_{tof} \approx$60 ps and a set of calorimeters.

The targets, C (561 mg/cm^2), Si (1170 mg/cm^2) and Pb (224 mg/cm^2) for ion collisions and a liquid hydrogen cylinder (length 20 cm) for elementary interactions, are positioned about 80 cm upstream from VTPC-1.

Pb beam particles are identified by means of their charge as seen by a helium gas-Cerenkov counter (S2') and p beam particles by a 2 mm scintillator (S2). Both of these are situated in front of the target. The study of C+C and Si+Si reactions is possible through the generation of a secondary fragmentation beam which is produced in a primary target (1 cm carbon) in the extracted Pb-beam. With the proper setting of the beam line magnets a large fraction of all $Z/A = 1/2$ fragments are transported to the NA49 experiment. On-line selection based on a pulse height measurement in a scintillator beam counter (S2) is used to select particles with $Z = 6$ (carbon) and $Z = 13, 14, 15$ (Al, Si, P). In addition, a measurement of the energy loss in beam position detectors (BPD-1,2,3 in Fig. 15) allows for a further selection in the off-line analysis. These detectors consist of pairs of proportional chambers and are placed along the beam line. They also provide a precise measurement of the transverse positions of the incoming beam particles.

For p beams, interactions in the target are selected by an anti-coincidence of the incoming beam particle with a small scintillation counter (S4) placed at the beam axis between the two vertex magnets. For p+p interactions at 158A GeV this counter selects a (trigger) cross section of 28.5 mb out of 31.6 mb of the total inelastic cross section. For Pb beams, an interaction trigger is provided by an anti-coincidence with a helium gas-Cerenkov counter (S3) directly behind the target. The S3 counter is used to select minimum bias collisions by requiring a reduction of the Cerenkov signal by a factor of about 6. Since the Cerenkov signal is proportional to Z^2, this requirement ensures that the Pb projectile has interacted with a minimal constraint on the type of interaction. This setup limits the triggers on non-target interactions to rare beam-gas collisions, the fraction of which proved to be small after cuts, even in the case of peripheral Pb+Pb collisions.

The centrality of the nuclear collisions is selected by use of information from a downstream calorimeter (VCAL), which measures the energy of the projectile spectator nucleons. The geometrical acceptance of the VCAL calorimeter is adjusted in order to cover the projectile spectator region by the setting of the collimator (COLL).

Details of the NA49 detector setup and performance of tracking software are described in [4].

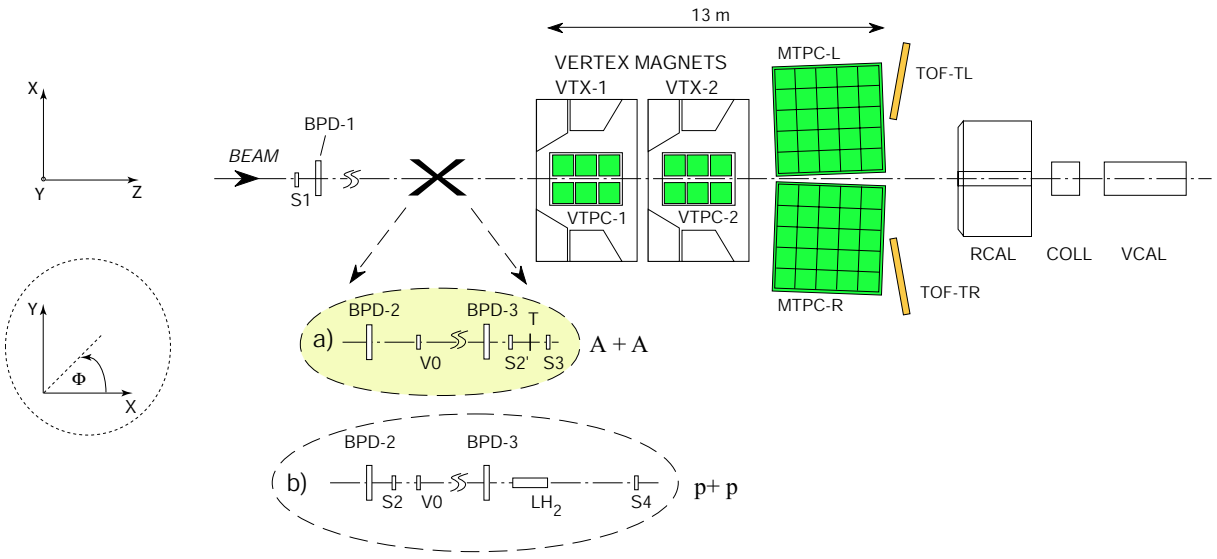

Figure 15: The experimental set–up of the NA49 experiment [4] with different beam definitions and target arrangements.

3.2 Stage I upgrades

For the first stage of data taking the following modifications or replacements of obsolete equipment of the existing NA49 facility are planned.

In the trigger system the beam defining counters have to be replaced. The trigger logics (based on NIM and CAMAC) needs to be modernized like its Lab-View control system.

The beam position detectors need to be refurbished (rewiring, new LV power supplies and shaper boxes).

The FASTBUS read-out of the time-of-flight detectors has to be replaced by a modern VME system.

The data acquisition system is based on the old VME/VSB systems. A repository of spare modules is required.

The existing on-line computers need to be replaced with up-to-date Linux machines. The raw data has to be transferred to the central data recording system of the CERN IT division.

Control and monitoring of the low voltage and gas system has to be migrated to a standard PC based system. The hardware of the gas system and the cooling systems of the TPCs need to be revised and upgraded.

The total material cost of the upgrades listed above is estimated to be 250 kSFR and the required manpower is 3.5 man-years.

In order to optimize the existing setup for the runs for the neutrino and cosmic-ray

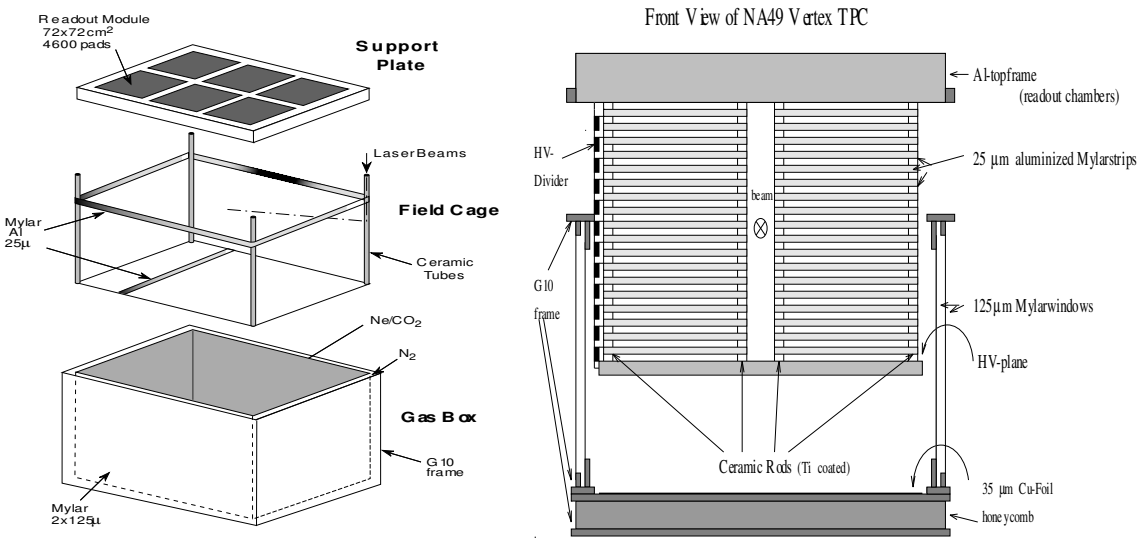

Figure 16: Schematic view of the Vertex TPCs mechanical construction.

physics needs the following modifications are under discussion.

In order to avoid complex trigger-bias corrections a simple trigger avoiding a beam veto in the downstream decision logic can be used. The most unbiased solution is to trigger with scintillator planes downstream of the TPCs covering the full acceptance of the secondary particles within the momentum and angular window of interest. Alternatively, a small scintillator telescope can be used which intercepts the non-interacting beam particles. A coincidence in this telescope selects interactions by vetoing the beam particle. The latter solution requires only a very small amount of hardware, but may induce some bias by over-vetoing. It will be investigated which of the two solutions is optimal. It is expected that these low-bias triggers have a relatively low purity. This is taken into account in the data taking needs.

The NA49 detector is equipped with a high-precision time-of-flight measurement system. This system is valuable to cross-check and calibrate the PID measurement based on dE/dx in the TPCs but has a limited acceptance. It is presently being investigated whether the addition of more TOF detectors will significantly improve the results. Especially in the low momentum region, where the dE/dx bands of pion, kaon and proton cross, an additional TOF measurement is useful. This region lies at sufficiently low β to allow PID by time-of-flight to be performed successfully.

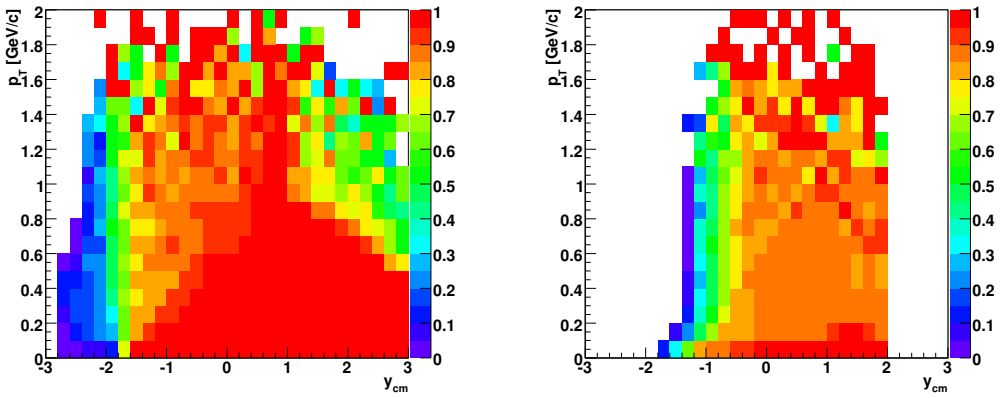

Figure 17: Geometrical acceptance in transverse momentum and rapidity of the TPCs after modifications of the geometry for collisions at 158A GeV (left) and 20A GeV (right). The beam and target rapidities are ± 2.91 and ± 2.08 at 158A and 20A GeV, respectively. The fraction of accepted vertex pions increase in comparison to the NA49 TPC configuration by $\approx$20% at 158A GeV and by $\approx$50% at 20A GeV.

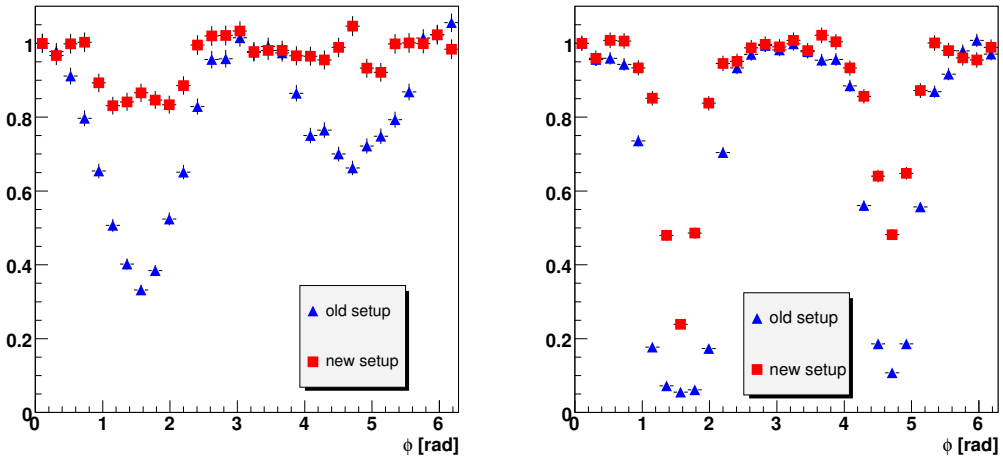

Figure 18: Geometrical acceptance in azimuthal angle for the rapidity interval $-1 < y < 0$ after (squares) and before (triangles) modification of the TPC geometry for collisions at 158A GeV (left) and 20A GeV (right).

3.3 Stage II upgrades

3.3.1 Increase of the Event Rate

The physics goals presented in Sections 2.2 and 2.3 require significant increase of the data rate in comparison to the NA49 system.

First investigations have demonstrated that it is possible to increase the event rate by a factor of about 20 by replacement of the TPC readout by an ALICE-like system while keeping the TPC front-end cards of NA49.

The higher beam rate requires besides the change of the DAQ system, the introduction of a vacuum beam pipe to minimize chamber loading effects of δ-electrons. Additionally fast beam position detectors have to be introduced.

3.3.2 Enlargement of the TPC Acceptance

In order to improve the performance of the detector for fluctuation and correlation measurements and to achieve the physics goals presented in Section 2.3 an enlargement of the TPC acceptance is necessary. This concerns in particular an increase of the acceptance in azimuthal angle and in the backward hemisphere.

This goal can be reached by reducing the gap between the sensitive volumes of the left and right readout chambers of the VTPC-1 and VTPC-2 detectors (see Fig. 16 for details of the vertex TPCs construction) from about 25 cm to 9 cm and moving the target closer to VTPC-1 (by about 60 cm). This together with the introduction of a vacuum beam pipe requires redesign of the field cages of the vertex TPCs.

The geometrical acceptance for charged vertex pions resulting from the above modifications is shown in Figs. 17 and 18 for collisions at 20A and 158A GeV. In Fig. 18 the new acceptance is compared with the acceptance of the standard NA49 setup. The fraction of registered vertex pions will be $\approx$75% and $\approx$90% for collisions at 20A and 158A GeV, respectively.

Other options to enlarge the acceptance of the NA49 facility are also under discussion. In particular, it is considered to add planar (between TPCs) and cylindrical (around target) GEM detectors in order to increase forward and backward rapidity coverage, respectively.

3.4 Stage III upgrades

3.4.1 Projectile Spectator Detector

The Projectile Spectator Detector (PSD) is meant to measure the number of non-interacting nucleons from a projectile nucleus in nucleus-nucleus collisions on an event-by-event basis which in turn allows to determine the number of nucleons participating in a reaction. The latter quantity is of key importance in the study of event-by-event fluctuations which are the focus of the future experimental searches for the critical point of strongly interacting matter and of the analysis of the properties of deconfinement.

The proposed PSD has two main features which distinguish it from the Zero Degree Calorimeters (ZDCs) commonly used by the current heavy ion experiments experiments at CERN and RHIC. First, it is the large size of the detector which is determined by the

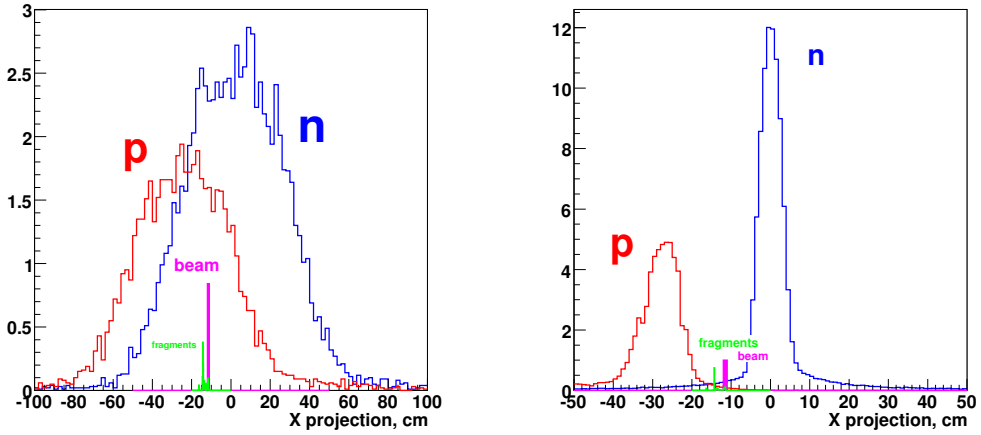

Figure 19: Spectator spot 20 m downstream of the interaction target: projection onto the (horizontal) X-axis for collision energies 10A GeV (left) and 100A GeV (right). The magnetic field is scaled proportional to the beam momentum.

spectator spots at the detector position in the required energy range, 10A-158A GeV. As seen in Fig. 19, the dimensions of the spectator spots increase strongly with decreasing energy due to an increasing spread caused by Fermi motion of the projectile spectators. This demands a large front (transverse) size ($\approx$ 2x1 m^2) calorimeter in contrast to compact ZDCs used at higher beam energies. Second, it is the required energy resolution which must be several times better than the typical resolution of ZDCs due to the challenging task of a precise measurement of the number of participants.

The main properties of the required detector are:

- a high energy resolution of the total energy of the projectile spectators ($\sigma(E)/E < 50/\sqrt{(E)}$) in a very broad energy range from 10 GeV to 30 TeV which should lead to a low uncertainty in the determination of the number of interacting nucleons even for peripheral collisions of heavy nuclei at low energies (below 10% for Pb+Pb collisions with 20 participant nucleons),

- a modular design, which should allow to optimize the detector geometry in accordance with the requirements defined by the collision energy as well as the target-PSD distance and the magnetic field used in the experiment, and provide the necessary reduction of systematic errors due to non-uniformity and leakage,

- a high granularity of the energy measurement, which will enable the separation of different contributions (protons, neutrons, fragments) and should allow the determination of the event reaction plane.

Challenging energy resolution, transverse uniformity as well as linearity and Gaussian shape of the detector signal are the critical parameters for the appropriate detector design. These requirements mandate a specific type of PSD, namely, the compensating hadron calorimeter. The concept of compensating calorimetry was intensively developed during the last years based on the understanding of the physical processes inside the hadron shower. The hadron shower in an absorber consists in reality of two components, one electromagnetic (e) and the other pure hadronic (h). The former originates from neutral pions produced in nuclear interactions and is the dominant source of the fluctuations. The energy sharing between the e and h components can be very different from event to event and depends mainly on the nature of the first interaction, which will produce (or not produce) π^0s. The equalization of the calorimeter response to the e and h components ($e/h = 1$ or compensation concept) eliminates one of the dominant sources of the energy fluctuation and hence improve the energy resolution of the calorimeter. The other advantages of compensating calorimeters are the linearity and the Gaussian shape of the detector signal. This concept was initially applied to uranium calorimeters and then generalized. Now this approach is successfully applied to calorimeters with iron and/or lead absorbers [76]. It was shown, that the compensating condition ($e/h = 1$) depends on the relative absorber/active medium thickness ratio and equals Fe:Scintillator=20 for iron absorber and Pb:Scintillator=4 for lead absorber. The lead/scintillator calorimeter is rather attractive due to the smaller compensating ratio and consequently smaller sampling fluctuation of the shower.

These general considerations were confirmed experimentally during the last few years. At present, there exist a few compensating lead/scintillator calorimeters with rather promising energy resolution [77, 78]. These designs together with preliminary Monte Carlo simulations indicate that the compensating lead/scintillator calorimeter meets all the requirements of our project and might be cheap enough in spite of the rather large required size.

The above considerations allow us to summarize the parameters of PSD modules as follows:
-energy resolution $< 50\%/\sqrt{(E)}$,
-transverse non-uniformity of the light collection $< 5\%$,
-full functionality in the energy range 10-30000 GeV,
-transverse dimensions of a single PSD module: 10x10 cm^2,
-longitudinal segmentation: 60 layers of lead and scintillator,
-lead thickness of one layer 16 mm,
-scintillator thickness of a single layer 4 mm,
-total length of a single module 120 cm (6 nuclear interaction lengths).

The key challenge in the development of the PSD detector is to establish a reliable method of light readout. Traditional usage of WLS plates and/or fibers with subsequent

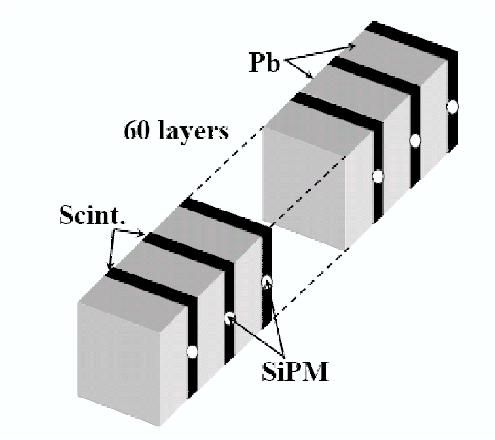

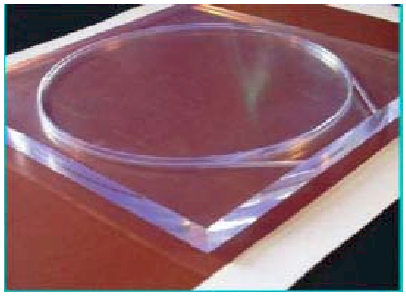

Figure 20: Top: PSD module: Pb-lead absorber, Scint.: scintillator plate with WLS fiber tile, SiPM: silicon photo-multiplier. Bottom: Photo of scintillator plate-WLS-tile unit. The WLS-fiber is situated in the circular groove and one fiber end is read out by the silicon photo-multiplier.

coupling to Photo Multiplier Tubes (PMT) has several problems, namely, Cerenkov radiation in plates/fibers, nuclear counting effect in PMTs, light transport over long distances (attenuation length, radiation effect, mechanical instability, etc.). Presently, the most advanced technique for the light readout is use of the tile WLS-fibers which are embedded in the scintillator plates. This method is used in all LHC experiments. It provides excellent performance including high light collection efficiency and uniformity along the the

scintillator plates. The light can be read out directly by silicon photo-multipliers (SiPM) coupled to the edges of the fiber-tiles. SiPMs are rather novel devices with very promising properties [79]. They are avalanche photo-diodes working in Geiger mode with internal gain up to $\approx$5x10^6. SiPMs have extremely compact dimensions of a few millimeters and hence can be inserted directly in the detector body. Due to the pixel structure, SiPMs have no nuclear counting effect, are sensitive to the single photo-electron signal and have remarkable energy resolution even for a signal from a few photoelectrons. The technology of SiPM production and their parameters have rapidly improved. Presently there are several experimental setups that use SiPMs for the light readout [80] including the hadron calorimeter prototype for the future International Linear Collider project.

The sketch of one PSD module is shown in Fig. 20. About 200 modules are required to fully cover the spectator spot at 10A GeV beam energy.

Further development of the PSD needs detailed simulation including realistic beam conditions, detector geometry and hadron shower propagation in the calorimeter. The optimization of the detector dimensions as well as of the longitudinal module segmentation must be done. Also, intensive R+D should be performed to study the light readout from the WLS fiber tiles and SiPMs. Nevertheless, the proposed concept of the PSD as a full compensating lead/scintillator calorimeter seems to be rather realistic and satisfies all the requirements of our project.

4 Physics Performance

4.1 Neutrino and Cosmic-Ray Physics Needs

In NA49 the TPCs perform the task of measuring the trajectories of particles and to contribute to the particle identification (PID) by dE/dx measurements. A time-of-flight (TOF) measurement system supplements the PID. In particular, the TOF provides a good measurement of the PID in the non-relativistic regime where the dE/dx–p curves of pions, protons, and kaons cross.

The acceptance of the Main TPCs and TOF detectors of the NA49 facility in the p–θ plane is shown in Fig. 21 for the magnetic field configuration used in running at 40A GeV. The identification of charged pions, kaons and protons by use of the dE/dx measurements in MTPCs is possible for $p >$ 3 GeV/c. At lower momenta ($1 < p < 3$ GeV/c) the identification is performed with the help of the TOF information. Comparing the acceptance needed for neutrino physics shown in Fig. 3 with the NA49 acceptance (Fig. 21), one notes that the NA49 detector is very well suited for the reference measurements required by the neutrino program.

The acceptance needed for the measurements motivated by the cosmic-ray physics is shown in Fig. 5. It is almost fully located in the forward hemisphere, $y > 0$, where y denotes the pion rapidity in the center of mass system. In Fig. 23 (below) the rapidity

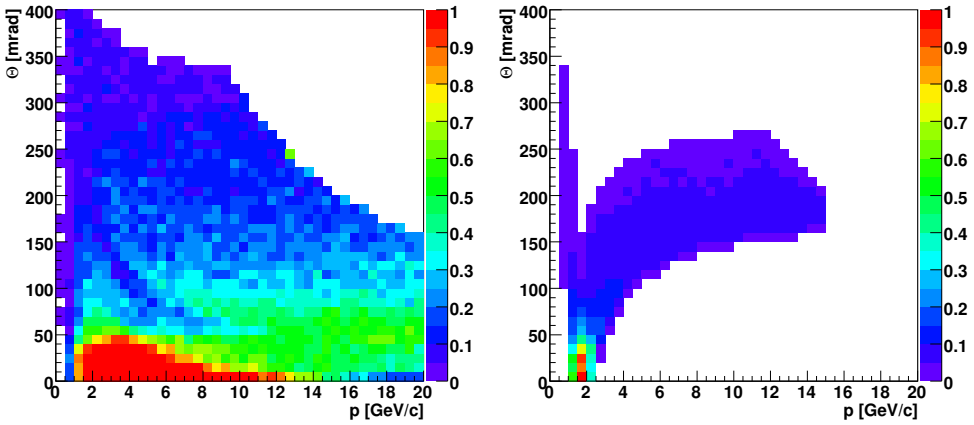

Figure 21: The acceptance of NA49 TPC (left) and TOF (right) detectors in the p–θ plane for hadrons for 40A GeV magnetic field configuration. The color of the fields indicates the relative acceptance of the detector at a given point in phase space.

spectra of identified hadrons measured at the SPS energies (20A-158A GeV) are presented. For all hadrons and at all energies the NA49 acceptance matches requirements of the cosmic-ray experiments.

Running Time

With the present performance of the NA49 DAQ the maximum number of events which can be recorded per spill is about 50. Using a ball-park number of 18 s cycle length of the SPS, the requirement of 2×10^6 triggers per setting, and an efficiency of the SPS of about 80% to obtain the statistics for one setting requires about 10 days. After the stage II DAQ upgrades the running time for a single configuration will be reduced to 1-2 days.

As the initial T2K runs are foreseen with 30 GeV/c protons we propose to start our measurements in 2007 by a one month run at 30 GeV/c. This will allow to collect basic data with two different target thicknesses. It will also include a setting-up period, and runs needed to study calibration and backgrounds. The further data on proton and pion interactions on carbon target required by the cosmic-ray (at 50 and 158 GeV/c) and neutrino (at 40 and 50 GeV/c) physics will be taken in 2008 after the increase of the event collection rate.

Conclusions

The NA49 detector is well suited to measure with high precision the identified hadron yields under conditions relevant for the T2K beam line as well as for the cosmic-ray ex-

periments. The measurements can be performed with only minor additions to the existing detector. There is a significant overlap between the data required by the neutrino and cosmic-ray experiments. The time scale is such that these measurements can be available at the start-up of T2K. These measurements would form an important contribution to the T2K (neutrino) as well as KASCADE and Pierre Auger (cosmic-ray) experiments, as a valuable addition to the present European efforts, *e.g.* the construction of the near detector (T2K) and the construction and running of the cosmic-ray experiments.

4.2 Reference p+p and p+A data

The detector upgrades planned for the stage II of data taking (see Section 3.3) will result in an increase of the event rate by a factor of about 20 and will lead to a significant improvement of the acceptance which will reach $\approx$ 75% at 20A GeV and $\approx$ 90% at 158A GeV

Thus within one month of p+p running at 158 GeV about $50 \cdot 10^6$ events with almost complete acceptance for charged particles will be registered. This will extend the p_T coverage for identified hadrons to $\approx$3 GeV/c and allow to study in detail fluctuations and correlations in large acceptance needed for a comparison with the corresponding data from A+A collisions (see Section 4.3).

4.3 Onset of deconfinement and critical point

In this section the performance of the upgraded detector (stage III) with respect to several important quantities for the future physics program with nuclear beams is discussed.

4.3.1 Inclusive spectra of identified hadrons

The future measurements of inclusive spectra of identified hadrons in C+C, Si+Si and In+In collisions at energies 10A-158A GeV are intended to be of similar statistical and systematic significance as the results for central Pb+Pb collisions obtained by NA49 in this energy range.

The lower multiplicity of hadrons produced in collisions of light and medium size nuclei as compared to Pb+Pb collisions will be approximately compensated by the higher (by a factor of about 20) number of registered events.

Typical systematic errors of the NA49 measurements of about 5-10% will be somewhat reduced by improved dE/dx resolution, tracking efficiency and reduction of the background due to relatively low multiplicity of hadrons produced in collisions of light and medium mass nuclei as well as use of the vacuum beam pipe.

In order to illustrate the quality of the expected results the transverse mass and rapidity spectra of identified hadrons measured by NA49 in central Pb+Pb collisions at the SPS energies are shown in Figs. 22 and 23.

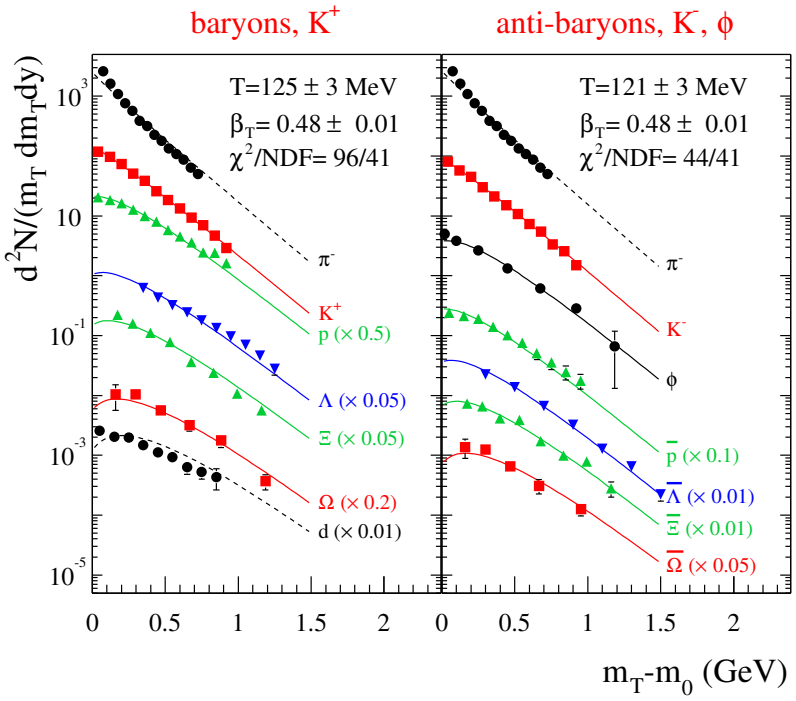

Figure 22: The transverse mass spectra of identified hadrons produced in central Pb+Pb collisions at 158A GeV [81]. Only statistical errors are plotted, the systematic errors are in the range 5-10%.

The precision of the expected measurements (5-10% for the particle yields and $\approx$ 10 MeV for T and $\langle m_T \rangle$) is sufficient (e.g. the yield ratios change be a factor of several, see Fig. 10) to answer the question how the transition from the anomalous energy dependence observed in central Pb+Pb collisions at SPS energies to the smooth behavior measured in p+p interactions looks like.

4.3.2 Fluctuations

One of the first proposed signals of the critical point of strongly interacting matter was a maximum of the transverse momentum fluctuations in the (collision energy)-(system size) plane [68]. NA49 performed the system size scan at 158A GeV and, in fact, a maximum was observed for collisions with a number of interacting nucleons of about 40 [70].

The experimental results are shown in Fig. 24, where the intensive fluctuation measure, ϕ_{P_T} is plotted against the mean number of interacting nucleons. The magnitude of the observed fluctuations, $\phi_{P_T} = 7 \pm 2$ MeV, is in approximate agreement with the predictions for the critical point, $\phi_{P_T} \approx 10$ MeV [82]. However, whether the measured fluctuations

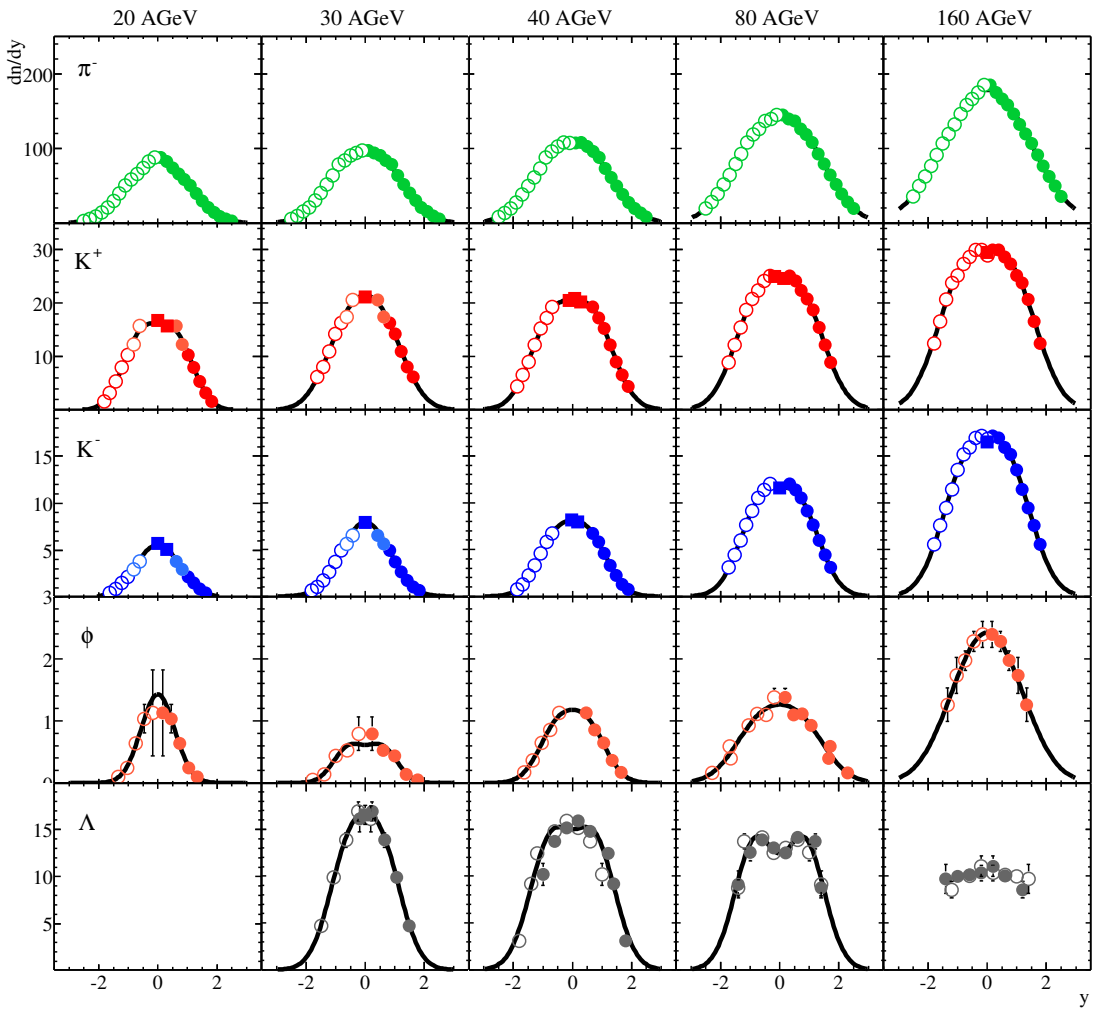

Figure 23: The rapidity spectra of identified hadrons produced in central Pb+Pb collisions at 20A, 30A, 40A, 80A and 158A GeV [81]. Only statistical errors are plotted, the systematic errors are in the range 5-10%.

signal the vicinity of the critical point remains an open question. This is mainly because systematic data on the energy dependence of this effect are missing. Only an observation of a maximum in the energy dependence can rule out several alternative explanations of the NA49 results.

The future measurements of p_T fluctuations in C+C, Si+Si and In+In collisions at 10A-158A GeV will clearly resolve this situation and possibly lead to the location of the critical point. Due to higher statistics, lower background and larger azimuthal angle

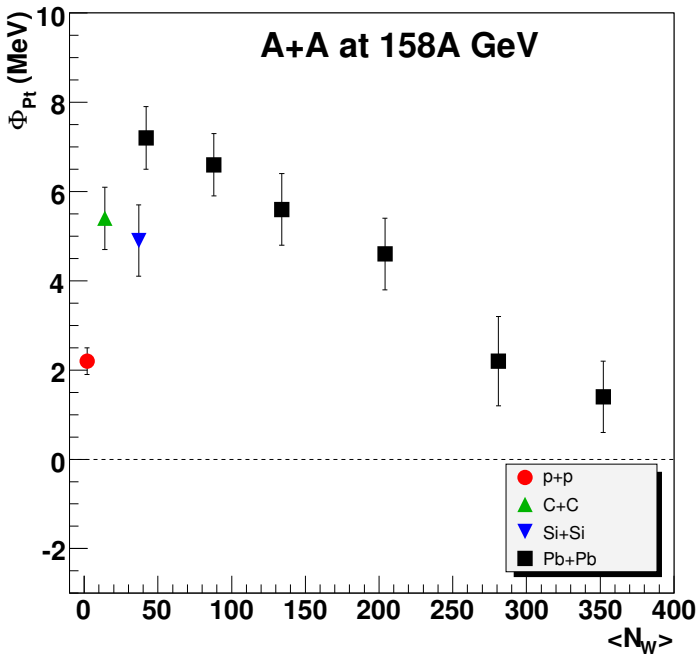

Figure 24: The measure of transverse momentum fluctuations ϕ_{p_T} versus mean number of interacting nucleons $\langle N_W \rangle$ for nuclear collisions at 158A GeV. The results for all charged hadrons are presented. Only statistical errors are plotted, the systematic errors are smaller than 1.6 MeV.

acceptance the statistical and systematic errors of the new measurements will be smaller by a factor of about 2. The new data will allow to perform measurements in a broad rapidity interval ($-1 < y < 3$) in which the magnitude of the critical fluctuations is expected to increase to about 20 MeV.

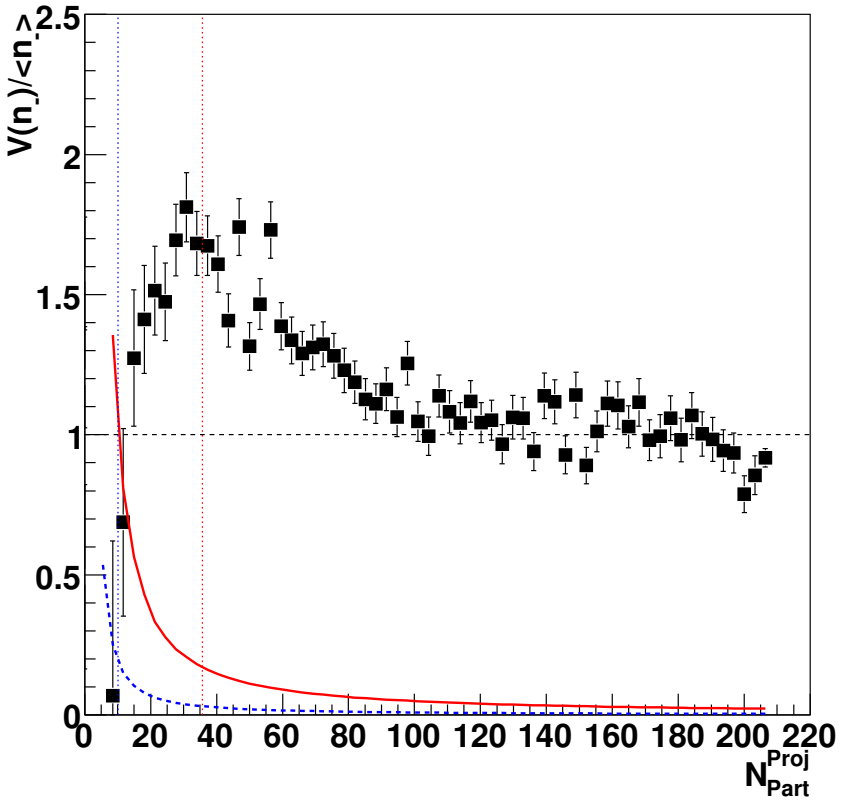

Figure 25: Scaled variance of the multiplicity distribution for negatively charged hadrons as a function of the number of projectile participants for Pb+Pb collisions at 158A GeV. The solid line shows the systematic error resulting from the performance of the NA49 Veto calorimeter. The dashed line indicates the systematic error estimate based on the parameters of the future Projectile Spectator Detector. The PSD detector will allow to establish the behavior of the scaled variance for peripheral collisions where a maximum is suggested by the present data.

Onset of deconfinement and the critical point are expected to lead to anomalies in the multiplicity fluctuations [53, 68]. In particular, the dispersion of the multiplicity distribution should increase by about 10-20% when crossing the energy domain in which the onset of deconfinement is located [53]. An experimental observation of these important effects is however not trivial. This is mainly because the measured multiplicity fluctuations are directly sensitive to the fluctuations in the number of interacting nucleons caused by event-by-event changes in the collision geometry. Thus a crucial experimental goal in the study of multiplicity fluctuations is to understand the influence of fluctua-

tions in the number of interacting nucleons. NA49 started pioneering investigations of the multiplicity fluctuations in nucleus-nucleus collisions at 158A GeV. The preliminary results suggest a large increase of the multiplicity fluctuations with decreasing centrality of Pb+Pb collisions. In Fig. 25 the scaled variance of the multiplicity distribution is plotted as a function of the number of interacting nucleons from the projectile nucleus. It was recently suggested [83] that the large fluctuations for peripheral collisions may be caused by mixing of particle sources from the projectile and target nuclei. This mixing is not present in existing string-hadronic models [84] and it can take place only at the very beginning of nucleus-nucleus collisions. Thus the study of multiplicity fluctuations as a function of collision centrality and system size provides a unique opportunity to test different models concerning the early stage of A+A collisions. Further systematic study of multiplicity fluctuations is thus urgently needed.

The influence of the fluctuations in the number of interacting nucleons from the projectile nucleus was removed by NA49 by the following procedure. First, the energy of the projectile spectator nucleons was measured for each event by the Veto calorimeter. The scaled variance was then calculated in narrow bins of the measured energy and thus only reduced fluctuations of the number of interacting nucleons are present in the event subsamples selected in this way. Secondly, the result was corrected for the remaining fluctuations of the number of interacting nucleons caused by the finite bin size, interaction of the projectile spectator nucleons in the detector material and the resolution of the Veto calorimeter. Unfortunately the latter two corrections are poorly known and this leads to a large (about 50% of the correction) systematic error on the scaled variance for peripheral collisions. The systematic error of the corrected scaled variance is shown in Fig. 25 by a solid line. It is larger than 0.2 for collisions with number of interacting projectile nucleons smaller than 35.

The large systematic error is caused mainly by an interplay between the strong non-uniformity of the Veto calorimeter response and the poorly known physics of the nuclear fragmentation processes. This error will be significantly reduced in the future measurements by use of the Projectile Spectator Detector and by a reduction of the material between the target and PSD due to the introduction of the vacuum beam pipe. The systematic error on the scaled variance expected for the future measurements is shown in Fig. 25 by a dashed line. It is smaller than 0.2 for collisions with the number of interacting projectile nucleons larger than 10.

The NA49 results indicate that the scaled variance depends on the acceptance. The acceptance of the NA49 detector is different for target and projectile hemispheres and changes with energy. This clearly leads to difficulties when system size and energy dependence of fluctuations is studied. The planned NA49 upgrades will significantly increase the acceptance available for fluctuation studies and thus will allow a reliable comparison of the results in target and projectile hemispheres and at different energies.

Similar to the multiplicity fluctuations, strangeness fluctuations are also considered

to be sensitive to the onset of deconfinement [53] and the critical point [85]. The first NA49 results indicate that dynamical strangeness fluctuations significantly increase at the low SPS energies, see Fig. 26. Is this related to the onset of deconfinement as predicted in [53]? To answer this question further experimental study is required. In particular, measurements with high statistics and lower systematic uncertainties in larger acceptance and energy range are needed.

The proposed future measurements meet all these requirements. At low energies the statistical errors will be smaller by a factor of about 3 due to high event statistics. The systematic error will be reduced because of the larger acceptance and lower track density. The acceptance will be increased and it will be approximately energy independent. Finally the measurement at $10A$ GeV will be crucial in getting more insight into the low energy behavior of strangeness fluctuations.

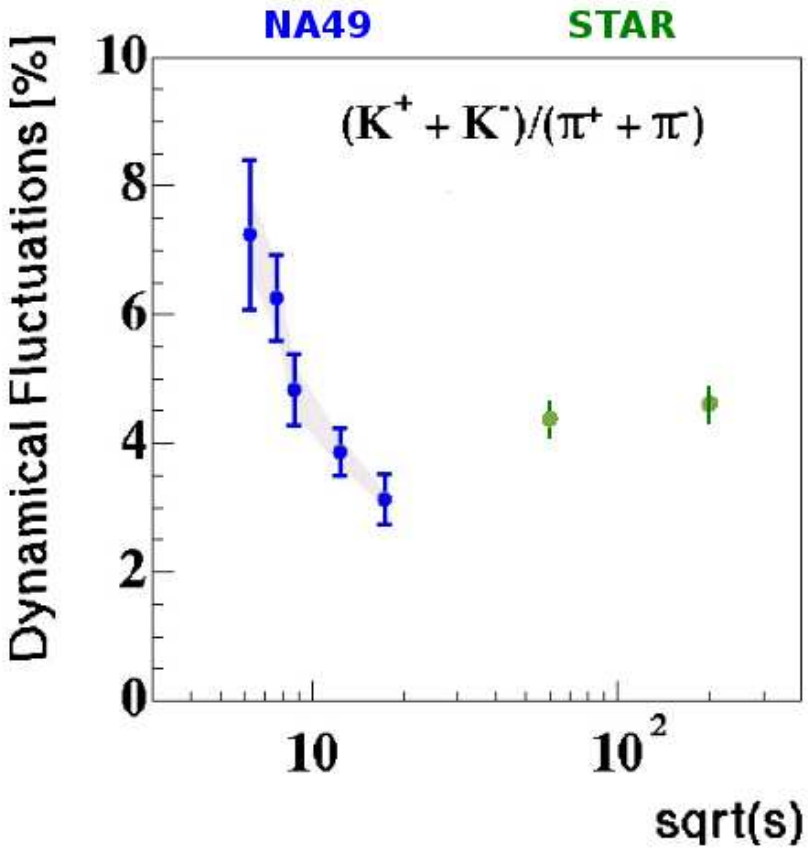

Figure 26: The energy dependence of dynamical strangeness fluctuations in central Pb+Pb (Au+Au) collisions at SPS and RHIC energies.

4.3.3 Anisotropic flow

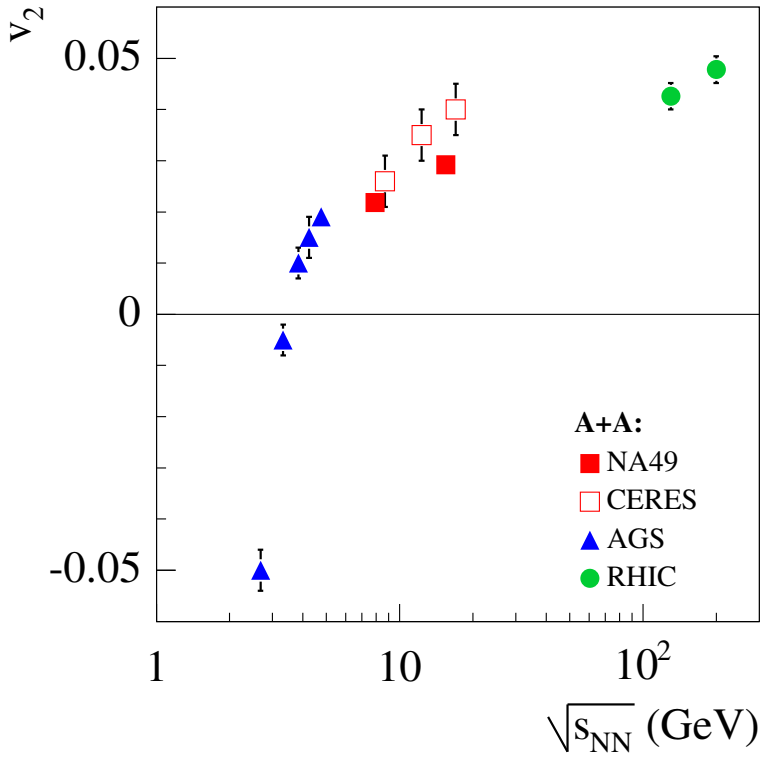

Figure 27: The energy dependence of elliptic flow of charged pions at mid-rapidity in Pb+Pb (Au+Au) collisions for mid-central events.

The energy dependence of anisotropic flow is considered to be sensitive to both the onset of deconfinement [54] and the critical point [86]. The two can be distinguished by separate measurements of the flow for mesons and baryons. In the case of the onset of deconfinement the flow of both mesons and baryons should be reduced [87], whereas the critical point should lead to a decrease of the baryon flow and an increase of the meson flow [86]. However, the existing data [88] are inconclusive on whether the expected effects are present in the CERN SPS energy range. The main experimental results are summarized in Figs. 27 and 28. The energy dependence of the v_2 parameter for pions in Pb+Pb (Au+Au) collisions is shown in Fig. 27. A rapid increase observed at low energies seems to weaken in the SPS energy range. In Fig. 28 the rapidity dependence of the elliptic flow parameter, v_2, of pions and protons is plotted for Pb+Pb collisions at 40A GeV. The results from the standard analysis suggest the reduction of v_2 for protons at mid-rapidity. This effect is, however, not observed in the results from the cumulant analysis and the

40A GeV data from NA49 are the only data on proton flow at low SPS energies. Thus the present data suggest the possibility of anomalies in the energy dependence of elliptic flow of mesons and baryons at the SPS energies, but they are too sparse to allow any firm conclusion.

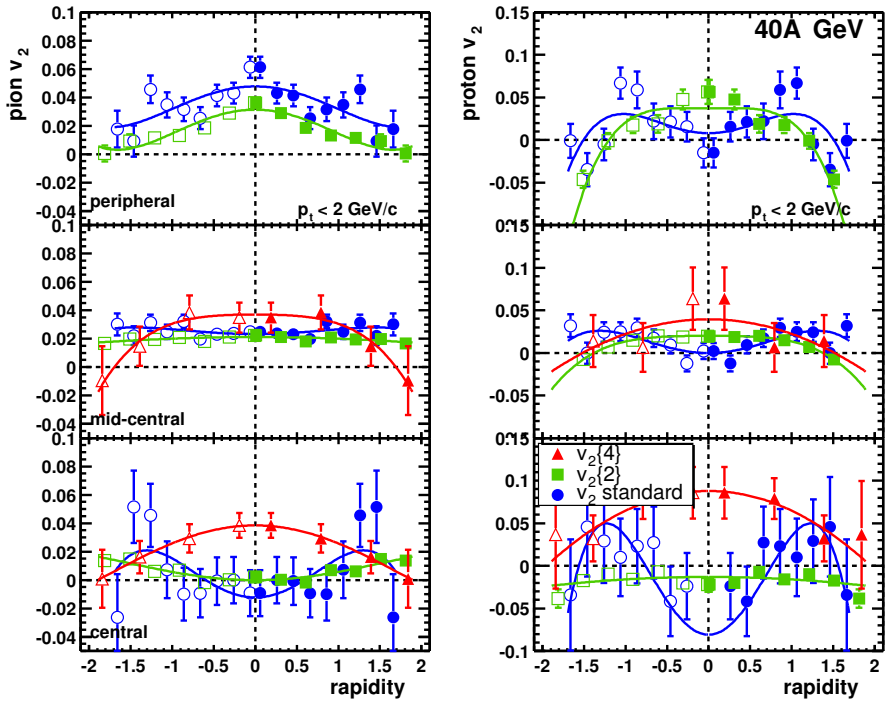

Figure 28: Elliptic flow of charged pions (left) and protons (right) obtained from the standard (v_2 standard) and cumulant ($v_2(2)$) methods as a function of the rapidity in Pb+Pb collisions at 40A GeV for three centrality bins. The open points have been reflected with respect to mid-rapidity. The solid lines are from polynomial fits.

The future measurements of In+In collisions at 10-158A GeV will allow to establish the energy dependence of the elliptic flow for mesons (charged pions and K^0_S mesons) and baryons (protons and Λ hyperons). For pions and protons the statistical resolution will be increased by a factor of about 2 in comparison to the NA49 results at 40A GeV and the systematic error will be reduced due to lower track multiplicity, lower background and higher acceptance in azimuthal angle (see Fig. 18).

The large event statistics of the new data will allow to measure elliptic flow of K^0_S mesons and Λ hyperons. First results on Λ elliptic flow were recently obtained by NA49 from a high statistics ($3 \cdot 10^6$ events) sample of Pb+Pb collisions at 158A GeV, see Fig. 29. The Λ multiplicity in In+In collisions is expected to be about half of that in

Pb+Pb interactions, and approximately energy independent in the SPS energy range like in Pb+Pb collisions. Thus the expected Λ multiplicity in $2 \cdot 10^6$ In+In events will be close to the Λ multiplicity in $1 \cdot 10^6$ Pb+Pb collisions. The results obtained from this statistics are also plotted in Fig. 29 to illustrate the feasibility of the Λ hyperon flow measurements in the future study

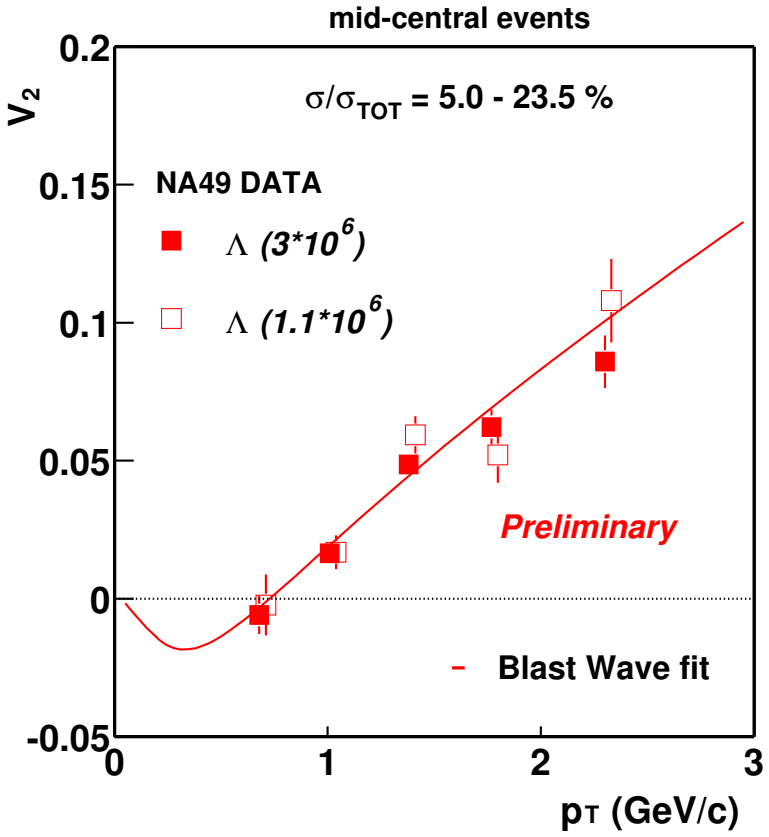

Figure 29: Elliptic flow of Λ hyperons as a function of the transverse momentum in mid-central Pb+Pb collisions at 158A GeV obtained using the full event sample of NA49 ($3 \cdot 10^6$) events and the reduced ($\approx 1 \cdot 10^6$) event sample which yields the same Λ hyperon statistics as expected in the future measurements.

The expected results on elliptic flow of mesons and baryons in In+In collisions at 10A-158A GeV will allow to establish the energy dependence of the v_2 parameter and therefore they will help to answer the question whether effects predicted for the onset of deconfinement and the critical point are present at the CERN SPS energies.

5 Beam requirements and expected event numbers

The beam requirements and the expected event numbers needed to reach the physics goals of the programme presented in this document are summarized below:

- 2006: 7 days of proton beam at 200 GeV;
  test run
- 2007: 30 days of proton beam at 30 GeV;
  $3 \cdot 10^6$ p+C events,
- 2008: 45 days of proton and pion beams at 30, 40, 50 and 158 GeV;
  $75 \cdot 10^6$ p+p, p+C and π+C events,
- 2009: 30 days of indium beam at 10A, 20A, 30A, 40A 80A, 158A GeV;
  $2 \cdot 10^6$ In+In events at each energy,
- 2010: 30 days of silicon beam at 10A, 20A, 30A, 40A 80A, 158A GeV;
  $2 \cdot 10^6$ Si+Si events at each energy,
- 2011: 30 days of carbon beam at 10A, 20A, 30A, 40A 80A, 158A GeV;
  $2 \cdot 10^6$ C+C events at each energy.

For the period 2009-2011 we also plan to request runs with the proton beams at energies between 10 GeV and 200 GeV (about 4 weeks per year) to continue study of p+p and p+A interactions started by the 2007 and 2008 runs.

6 Summary

A programme to study hadron production in collisions of protons and nuclei at the CERN SPS is proposed. It consists of three subjects:

- measurements of hadron production in nucleus-nucleus collisions, in particular fluctuations and long range correlations, with the aim to identify properties of the onset of deconfinement and search for the critical point of strongly interacting matter,

- measurements of hadron production in proton-proton and proton-nucleus interactions needed as reference data for better understanding of nucleus-nucleus reactions; in particular correlations, fluctuations and high transverse

momenta will be the focus of this study,

- measurements of hadron production in hadron-nucleus interactions needed for neutrino and cosmic-ray experiments.

The measurements should be performed by the upgraded NA49 apparatus in the period 2007-2011.

References

[1] R. Aymar et al., Phys. Rept. **403-404**, 1 (2004).

[2] J. Dainton et al., [The CERN SPS and PS Committee], CERN–SPSC–2005–010, SPSC–M–730 (2005).

[3] J. Bartke et al., *A new experimental programme with nuclei and proton beams at the CERN SPS*, CERN-SPSC-2003-038(SPSC-EOI-01) and presentations at the Villars workshop 2004.

[4] S. Afanasev *et al.* [NA49 Collaboration], Nucl. Instrum. Meth. A **430**, 210 (1999).

[5] C. Alt *et al.* [NA49 Collaboration], Phys. Rev. Lett. **94**, 052301 (2005) [arXiv:nucl-ex/0406031] and P. Dinkelaker [NA49 Collaboration], J. Phys. G **31**, S1131 (2005).

[6] C. Alt, arXiv:hep-ex/0510009.

[7] S. V. Afanasiev *et al.* [The NA49 Collaboration], Phys. Rev. C **66**, 054902 (2002) [arXiv:nucl-ex/0205002].

[8] M. Gazdzicki *et al.* [NA49 Collaboration], J. Phys. G **30**, S701 (2004) [arXiv:nucl-ex/0403023].

[9] M. Gazdzicki and M. I. Gorenstein, Acta Phys. Polon. B **30**, 2705 (1999) [arXiv:hep-ph/9803462].

[10] M. C. Gonzalez-Garcia and Y. Nir, Rev. Mod. Phys. **75**, 345 (2003) [arXiv:hep-ph/0202058].

[11] Y. Itow *et al.*, KEK report 2001-4.

[12] D. Ayres *et al.*, FNAL-P-929 (2002).

[13] P. Zucchelli, Phys. Lett. B **532**, 166 (2002).

[14] M.G. Catanesi *et al.*, HARP Collaboration, Measurement of the production cross-section of positive pions in p–Al collisions at 12.9 GeV/c, Nuclear Physics B **732**, 1 (2006).

[15] J. R. Sanford and C. L. Wang, Brookhaven National Laboratory, AGS internal report, 1967 (unpublished); C. L. Wang, Phys. Rev. Lett. **25**, 1068 (1970); ibid. **25**, 1536(E) (1970).

[16] M.H. Ahn *et al.*, K2K Collaboration, *Phys. Rev. Lett.* **90**, 041801 (2003);
M.H. Ahn *et al.*, K2K Collaboration, *Phys. Lett.* **B 511**, 178 (2001).

[17] E. Aliu *et al.*, K2K Collaboration, *Phys. Rev. Lett.* **94**, 081802 (2005).

[18] Y. Sugaya *et al.*, Nucl. Phys. A **634** (1998) 115.

[19] I. A. Vorontsov *et al.*, ITEP-11-1988.

[20] I. A. Vorontsov *et al.*, ITEP-85-1983.

[21] T. Abbott *et al.*, E-802 Collaboration, Phys. Rev. D **45** (1992) 3906.

[22] Y. Cho *et al.*, Phys. Rev. D **4**, 1967 (1971).

[23] A. Haungs, H. Rebel, and M. Roth, Rept. Prog. Phys. **66**, 1145 (2003).

[24] R. Engel and H. Klages, Comptes Rendus Physique **5**, 505 (2004).

[25] A. Bhattacharjee and G. Sigl, Phys. Rep. **327**, 109 (2000).

[26] R. Engel, Nucl. Phys. B (Proc. Suppl.) **122**, 40 (2003).

[27] T. Antoni *et al.* (KASCADE Collab.), Nucl. Instrum. Meth. A **513**, 490 (2003).

[28] J. Abraham *et al.* (Pierre Auger Collab.), Nucl. Instrum. Meth. A **523**, 50 (2004).

[29] T. Antoni *et al.* (KASCADE Collab.), Astropart. Phys. **24**, 1 (2005) and astro-ph/0505413.

[30] A. Fasso *et al.*, Proceedings of the Workshop on Simulating Accelerator Radiation Environments, Los Alamos, p. 134, 1992.

[31] M. Bleicher *et al.*, J. Phys. G: Nucl. Part. Phys. **25**, 1859 (1999).

[32] H. Fesefeldt, preprint PITHA-85/02, RWTH Aachen, 1985.

[33] N. N. Kalmykov, S. Ostapchenko, and A. I. Pavlov, Nucl. Phys. B (Proc. Suppl.) **52**, 17 (1997).

[34] H.-J. Drescher, M. Bleicher, S. Soff, and H. Stoecker, Astropart. Phys. **21**, 87 (2004) [arXiv:astro-ph/0307453].

[35] P. Sommers (Pierre Auger Collab.), astro-ph/0507150 to appear in Proc. of 29th ICRC, Pune, India, 3-11 Aug 2005.

[36] J. Knapp, D. Heck, and G. Schatz, in Wissenschaftliche Berichte FZKA 5828, Forschungszentrum Karlsruhe, 1996.

[37] R. Engel, T. K. Gaisser, and T. Stanev, Prepared for 29th International Symposium on Multiparticle Dynamics (ISMD 99), Providence, Rhode Island, 8-13 Aug 1999.

[38] H.-J. Drescher and G. R. Farrar, Astropart. Phys. **19**, 235 (2003) [arXiv:hep-ph/0206112].

[39] C. Meurer, J. Blumer, R. Engel, A. Haungs, and M. Roth, arXiv:astro-ph/0512536, to appear in Proc. of Int. Conference "From Colliders to Cosmic Rays" (C2CR 2005), Prague, Czech Rep., 7-13 Sep 2005.

[40] T. Eichten et al., Nucl. Phys. B **44**, 333 (1972); W.F. Baker et al., Phys. Rev. Lett. **7**, 101 (1961); D. Dekkers et al., Phys. Rev. B **137**, 962 (1965); R.A. Lundy et al., Phys. Rev. Lett. **14**, 504 (1965); J.V. Allaby et al., CERN Yellow Report 70-12 (1970); Y. Cho et al., Phys. Rev. D **4**, 1967 (1971); D. Antreasyan et al., Phys. Rev. D **19**, 764 (1979); D.S. Barton et al., Phys. Rev. D **27**, 2580 (1983); T. Abbott et al. (E-802 Collab.), Phys. Rev. D **45**, 3906 (1992).

[41] A. Laszlo and T. Schuster *et al.* [NA49 Collaboration], QM2005, Budapest 2005.

[42] E. W. Beier *et al.*, Phys. Rev. D**18**, 2235 (1978).

[43] S. R. Blattnig *et al.*, Phys. Rev. D**62**, 094030 (2000).

[44] B. Alper et al., Nucl. Phys. B**100**, 237 (1975).

[45] D. Antreasyan et al., Phys. Rev. D**19**, 764, (1979).

[46] V.V. Abramov et al., Nucl. Phys. B**173**, 348 (1980).

[47] V.V. Abramov et al., ZETFP **33**, 304 (1981).

[48] U. W. Heinz and M. Jacob, arXiv:nucl-th/0002042, J. Rafelski and B. Muller, Phys. Rev. Lett. **48**, 1066 (1982) [Erratum-ibid. **56**, 2334 (1986)], T. Matsui and H. Satz, Phys. Lett. B **178**, 416 (1986), F. Becattini, L. Maiani, F. Piccinini, A. D. Polosa and V. Riquer, arXiv:hep-ph/0508188.

[49] I. Arsene *et al.* [BRAHMS Collaboration], Nucl. Phys. A **757**, 1 (2005) [arXiv:nucl-ex/0410020], B. B. Back *et al.*, Nucl. Phys. A **757**, 28 (2005) [arXiv:nucl-ex/0410022], J. Adams *et al.* [STAR Collaboration], Nucl. Phys. A **757**, 102 (2005) [arXiv:nucl-ex/0501009], K. Adcox *et al.* [PHENIX Collaboration], Nucl. Phys. A **757**, 184 (2005) [arXiv:nucl-ex/0410003],

[50] M. I. Gorenstein, M. Gazdzicki and K. A. Bugaev, Phys. Lett. B **567**, 175 (2003) [arXiv:hep-ph/0303041].

[51] Y. Hama, F. Grassi, O. Socolowski, T. Kodama, M. Gazdzicki and M. Gorenstein, Acta Phys. Polon. B **35**, 179 (2004).

[52] E. L. Bratkovskaya *et al.*, Phys. Rev. C **69**, 054907 (2004) [arXiv:nucl-th/0402026], J. Cleymans and K. Redlich, Phys. Rev. C **60**, 054908 (1999) [arXiv:nucl-th/9903063].

[53] M. Gazdzicki, M. I. Gorenstein and S. Mrowczynski, Phys. Lett. B **585**, 115 (2004) [arXiv:hep-ph/0304052] and M. I. Gorenstein, M. Gazdzicki and O. S. Zozulya, Phys. Lett. B **585**, 237 (2004) [arXiv:hep-ph/0309142].

[54] J.-Y. Ollitrault, Phys. Rev. D **46**, 229 (1992), P. F. Kolb, J. Sollfrank and U. W. Heinz, Phys. Rev. C **62**, 054909 (2000) [arXiv:hep-ph/0006129].

[55] J. Cleymans and K. Redlich, Nucl. Phys. A **661**, 379 (1999) [arXiv:nucl-th/9906065].

[56] P. Braun-Munzinger, K. Redlich and J. Stachel, arXiv:nucl-th/0304013.

[57] F. Becattini and U. W. Heinz, Z. Phys. C **76**, 269 (1997) [Erratum-ibid. C **76**, 578 (1997)] [arXiv:hep-ph/9702274] and F. Becattini, M. Gazdzicki and J. Sollfrank, Eur. Phys. J. C **5**, 143 (1998) [arXiv:hep-ph/9710529].

[58] K. Rajagopal and F. Wilczek, arXiv:hep-ph/0011333.

[59] M. A. Stephanov, arXiv:hep-ph/0402115.

[60] F. Karsch, J. Phys. G **31**, S633 (2005) [arXiv:hep-lat/0412038].

[61] S. D. Katz, arXiv:hep-ph/0511166.

[62] F. Becattini, J. Manninen and M. Gazdzicki, arXiv:hep-ph/0511092.

[63] M. I. Gorenstein, M. Gazdzicki and W. Greiner, arXiv:nucl-th/0505050.

[64] N. G. Antoniou, Y. F. Contoyiannis, F. K. Diakonos, A. I. Karanikas, C. N. Ktorides, Nucl. Phys. A **693**, 799 (2001), N. G. Antoniou, F. K. Diakonos, G. Mavromanolakis, Nucl. Phys. A **761**, 149 (2005)

[65] Y. Hatta and T. Ikeda, Phys. Rev. D **67**, 014028 (2003) [arXiv:hep-ph/0210284].

[66] Z. Fodor and S. D. Katz, JHEP **0404**, 050 (2004) [arXiv:hep-lat/0402006].

[67] C. R. Allton *et al.*, Phys. Rev. D **71**, 054508 (2005) [arXiv:hep-lat/0501030].

[68] M. A. Stephanov, K. Rajagopal and E. V. Shuryak, Phys. Rev. D **60**, 114028 (1999) [arXiv:hep-ph/9903292].

[69] C. Alt *et al.* [NA49 Collaboration], Phys. Rev. C **68**, 034903 (2003) [arXiv:nucl-ex/0303001].

[70] T. Anticic *et al.* [NA49 Collaboration], Phys. Rev. C **70**, 034902 (2004) [arXiv:hep-ex/0311009].

[71] M. Rybczynski *et al.* [NA49 Collaboration], J. Phys. Conf. Ser. **5**, 74 (2005) [arXiv:nucl-ex/0409009].

[72] C. Roland *et al.* [NA49 Collaboration], J. Phys. G **30**, S1381 (2004) [arXiv:nucl-ex/0403035].

[73] A. B. Kurepin *et al.*, JETP Lett. **47**, 17 (1988).

[74] G. Stephans, Proceedings of the Quark Matter 2005, August 2005, Budapest, Hungary.

[75] T. Satogata, private communication.

[76] R. Wigmans, NIMA259(1987) 389-429

[77] G. A. Alekseev, *et al.*, NIM **A461** (2001) 381-383

[78] Y. Fujii, NIM **A453** (2000) 237-241

[79] I. Britvitch, *et al.*, NIM **A535** (2004) 523-527

[80] A. Akindinov, *et al.*, NIM **A539** (2005) 172-176

[81] S. V. Afanasiev *et al.*, Nucl. Phys. A **715**, 161 (2003) [arXiv:nucl-ex/0208014].

[82] M. A. Stephanov, Phys. Rev. D **65**, 096008 (2002) [arXiv:hep-ph/0110077].

[83] M. Gazdzicki and M. Gorenstein, arXiv:hep-ph/0511058.

[84] V. P. Konchakovski, S. Haussler, M. I. Gorenstein, E. L. Bratkovskaya, M. Bleicher and H. Stoecker, arXiv:nucl-th/0511083.

[85] R. Stock, arXiv:hep-ph/0404125.

[86] E. Shuryak, arXiv:hep-ph/0504048.

[87] E. L. Bratkovskaya *et al.*, arXiv:nucl-th/0401031.

[88] C. Alt *et al.* [NA49 Collaboration], Phys. Rev. C **68**, 034903 (2003) [arXiv:nucl-ex/0303001].